

Forward Physics: An Experimental Perspective

Prof Paul Newman
(University of Birmingham)



H1, ATLAS, LHeC, ePIC experiments

(please call me Paul)

Email: p.r.newman@bham.ac.uk

Midsummer School in QCD
Saariselkä, Finland
June 2024

Lecture 2: Soft Forward Physics &
Diffraction in proton-proton
Collisions

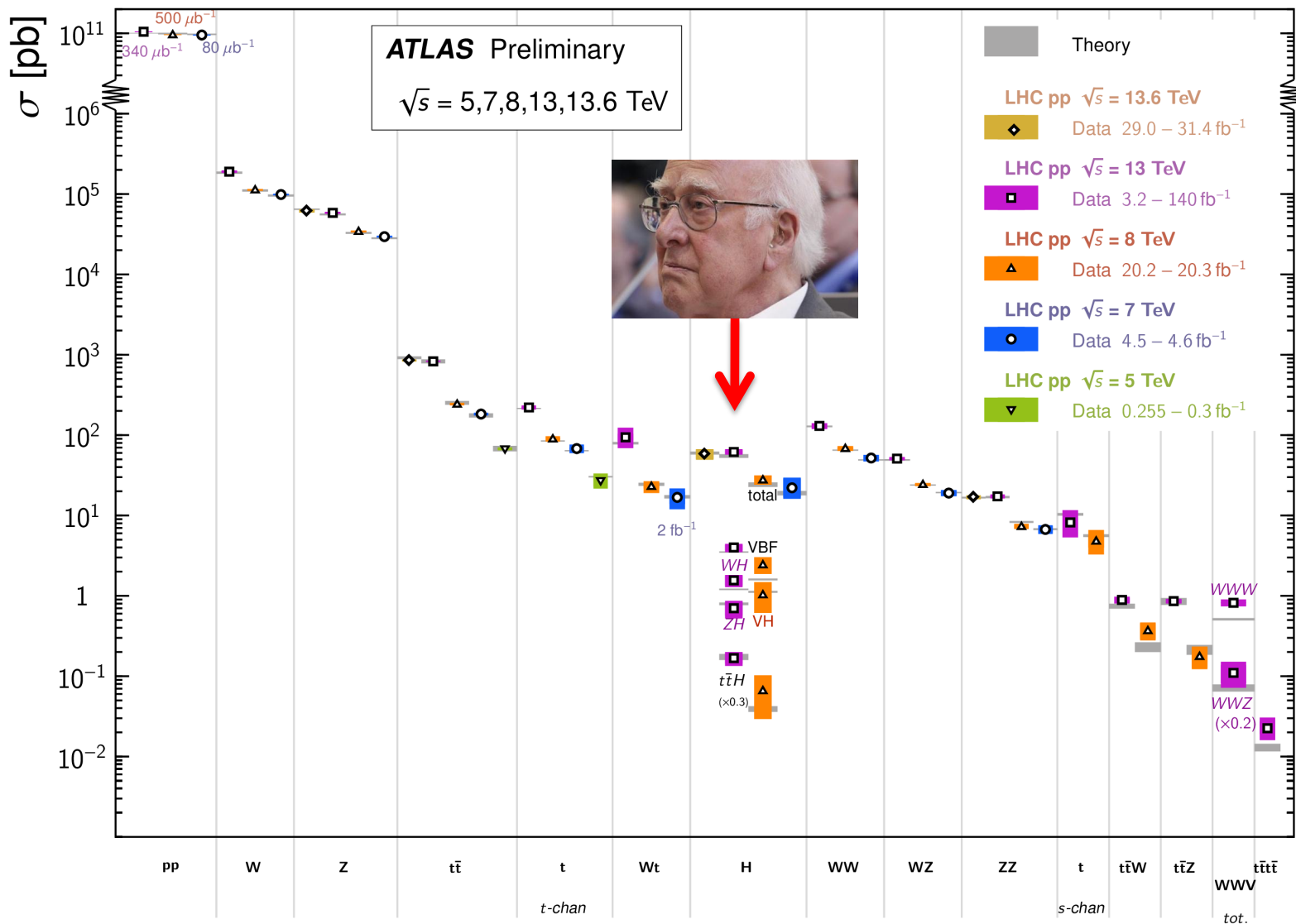
Lecture 2

- Minimum Bias LHC Data → Features of Non-Diffractive Data
- Experimental methods for processes with intact protons
- Elastic scattering at the LHC
- Single Diffractive dissociation at the LHC

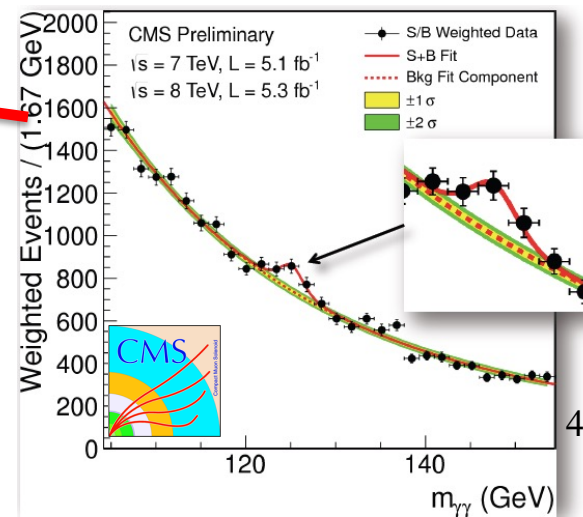
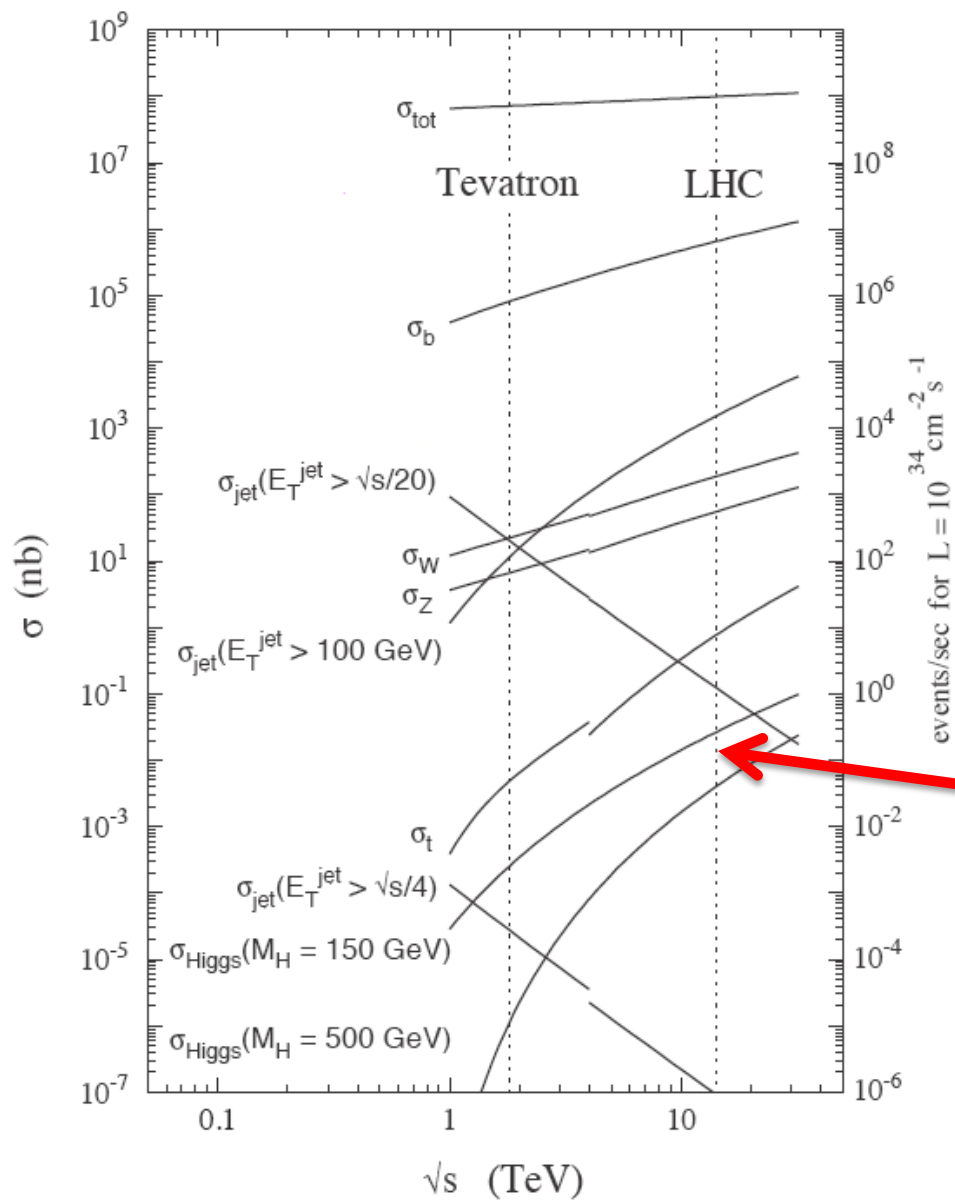
LHC: Exploring the ultra-rare at the Energy Frontier

Standard Model Total Production Cross Section Measurements

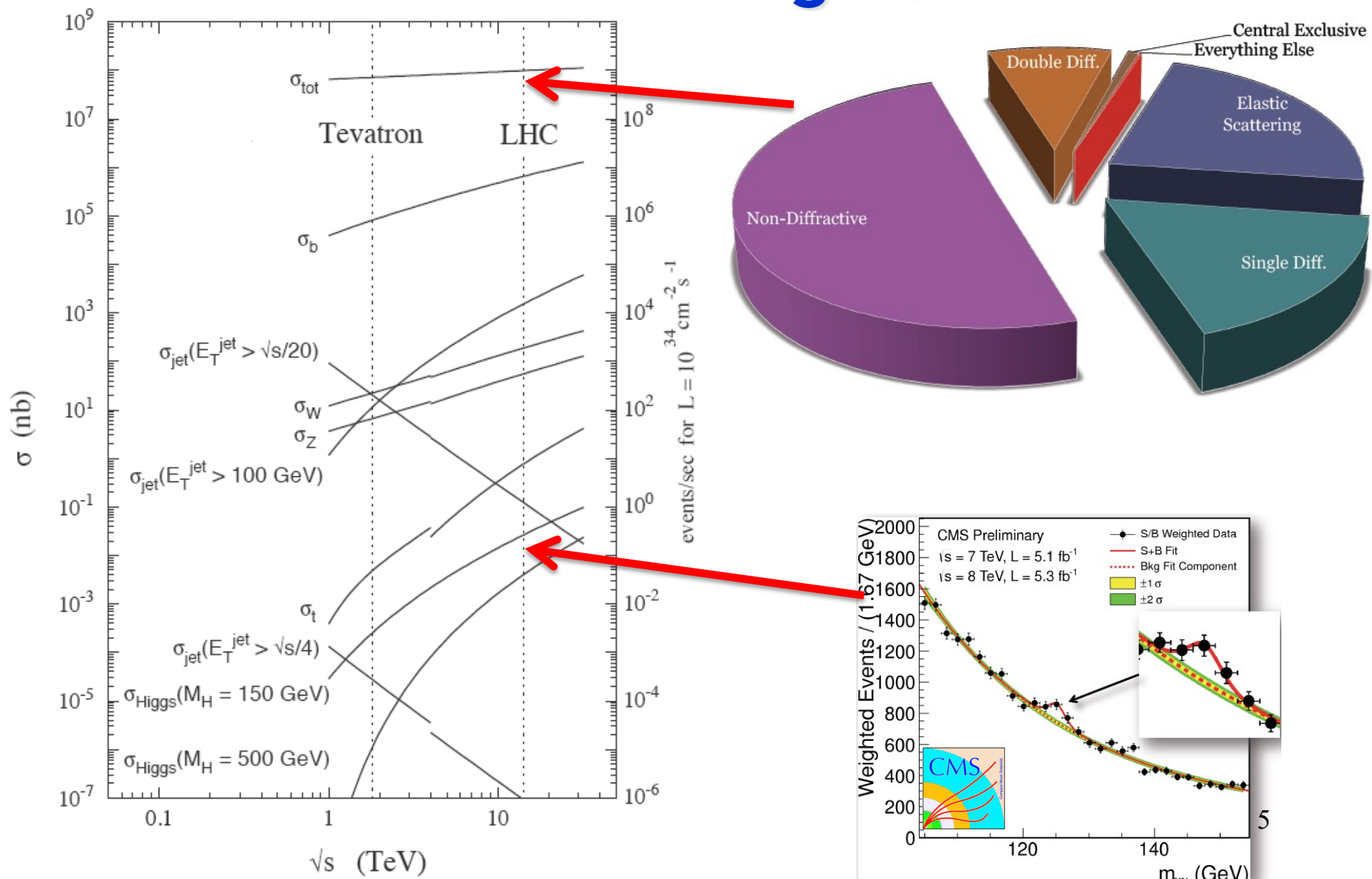
Status: October 2023



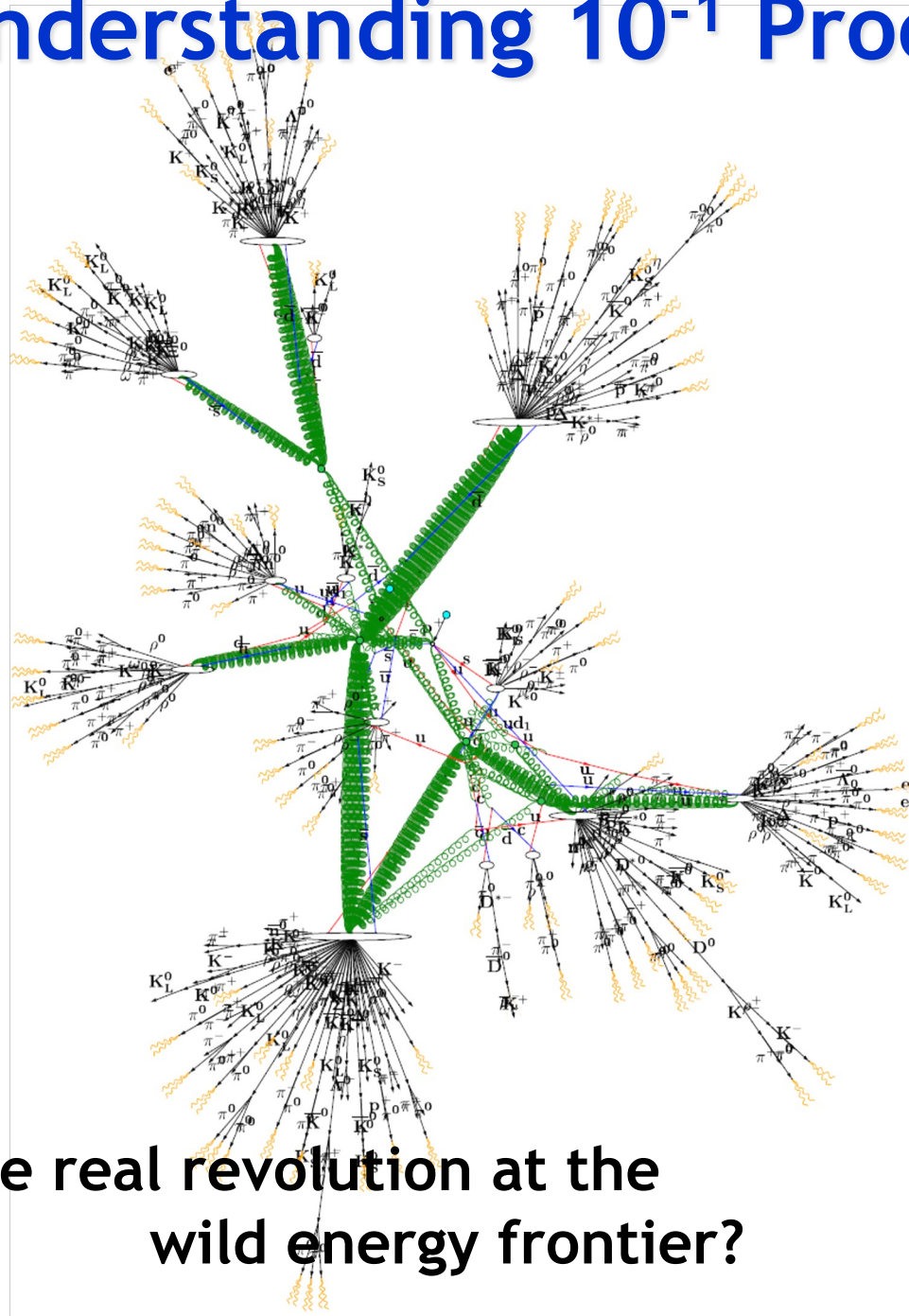
But what usually happens when hadrons collide at large \sqrt{s} ?



But what usually happens when hadrons collide at large \sqrt{s} ?



Understanding 10^{-1} Processes is Hard!

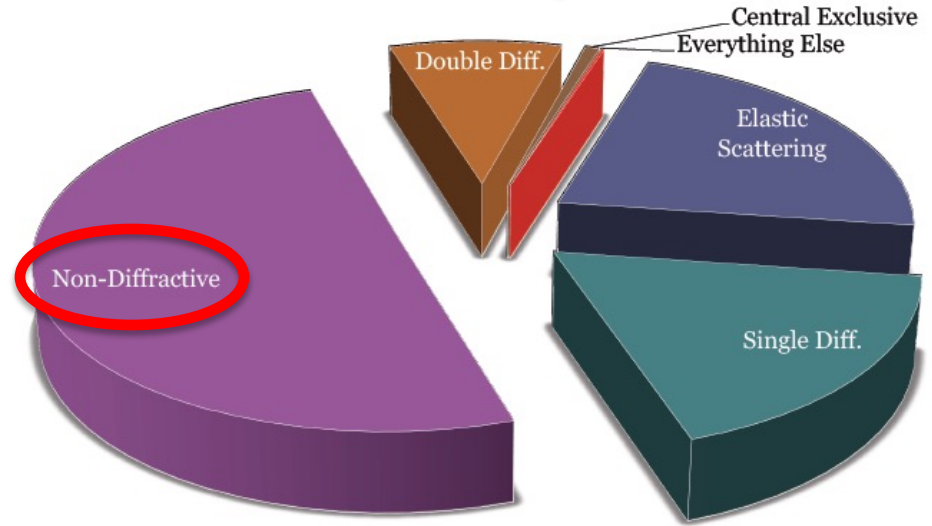
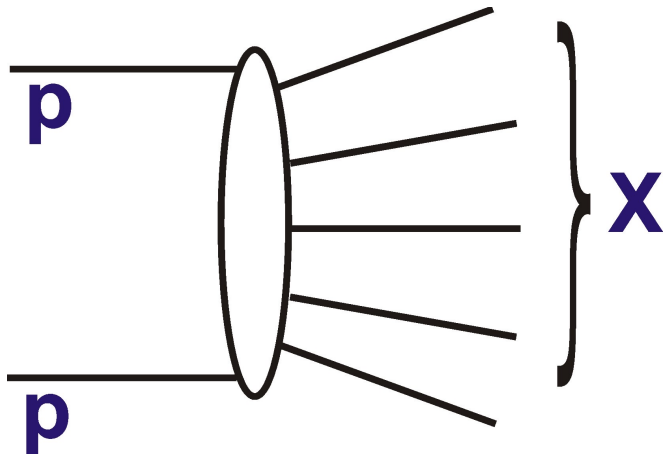


“minimum bias”
pp event in
PYTHIA8
at $\sqrt{s}=7$ TeV,
visualised
using MCViz

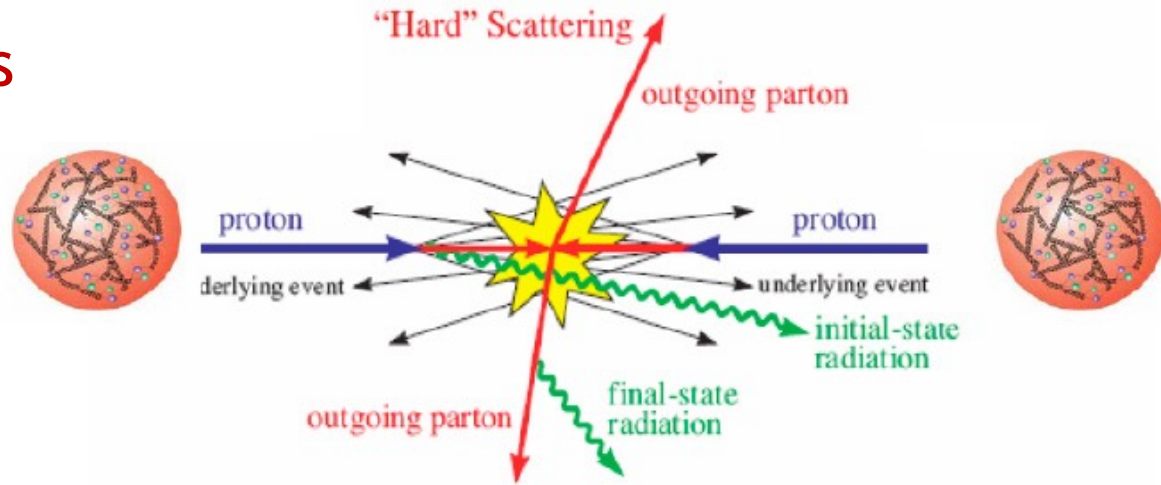
... the real revolution at the
wild energy frontier?



The bulk: soft non-diffractive processes



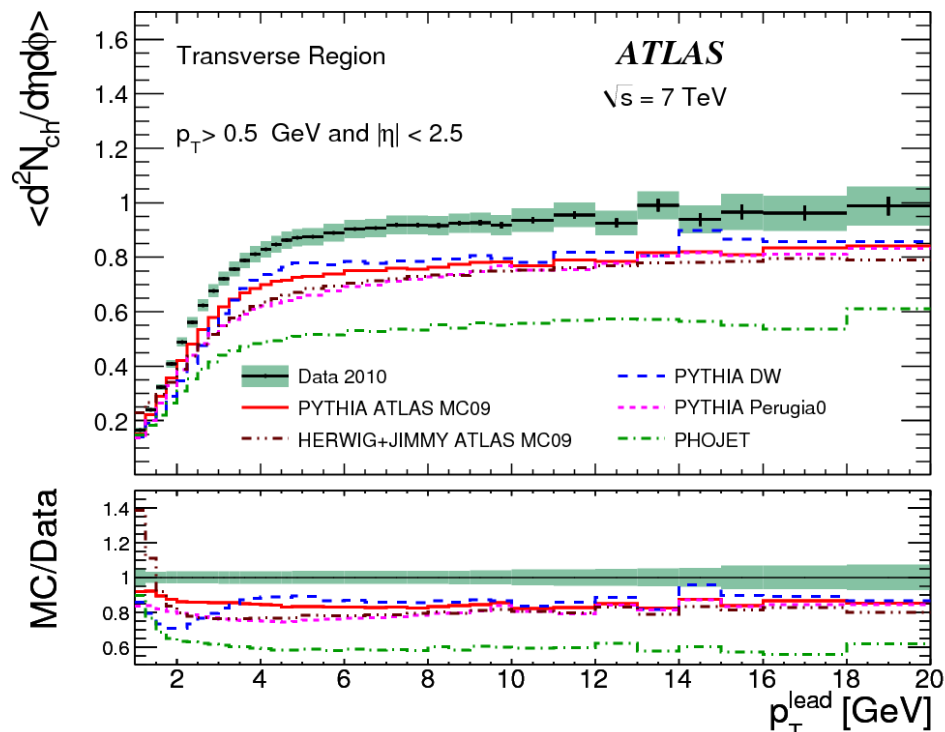
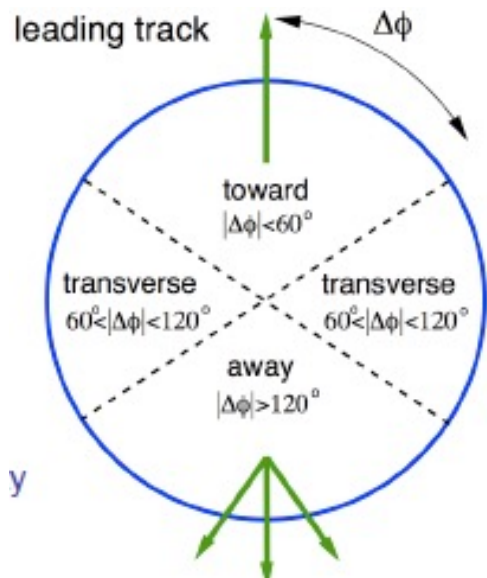
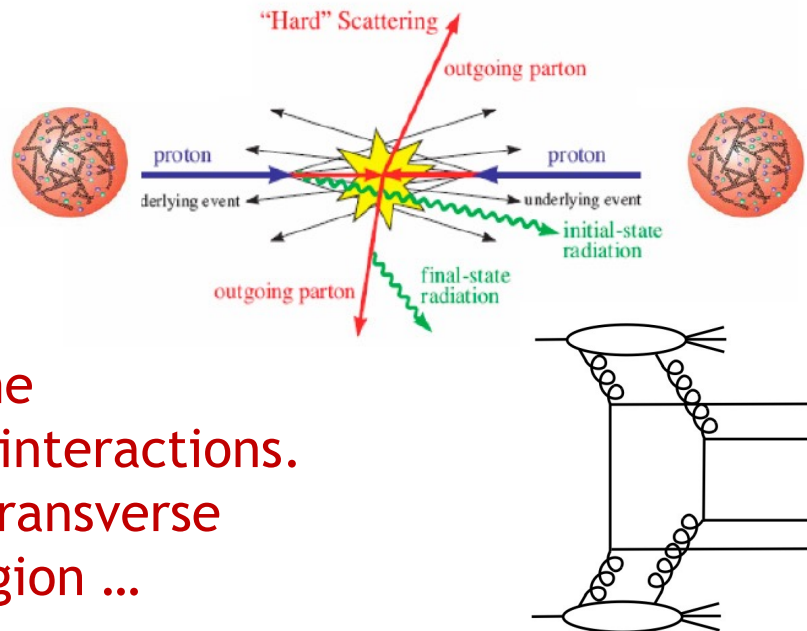
Complicated! ... and non-perturbative aspects not ignorable even for hard scatterings ...



The “underlying event”: originates from beam remnants and multiple soft and hard scatterings

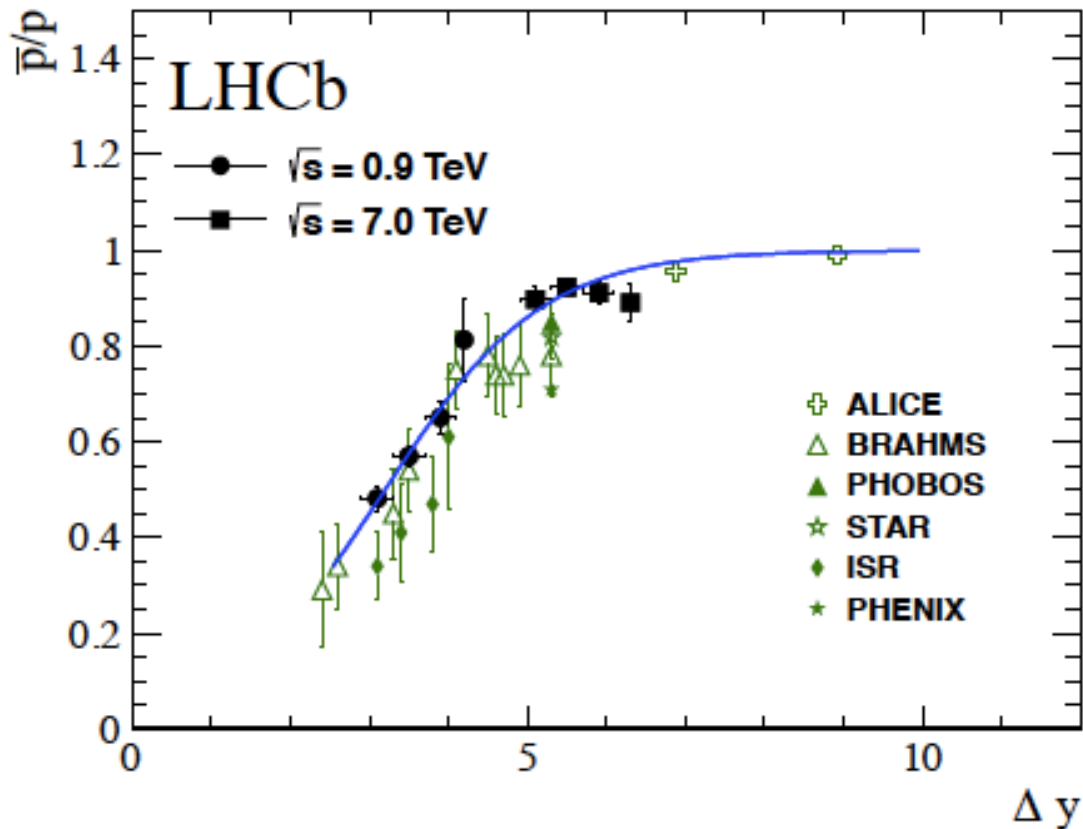
Evidence for Underlying Event / Multi-parton Scattering

- Region transverse to hard scattering plane particularly sensitive to multiple (parton) interactions.
- Pre-LHC MC models predicted too little transverse activity and jettiness in $\Delta\phi \sim 180^\circ$ away region ...



Complex Dynamics!

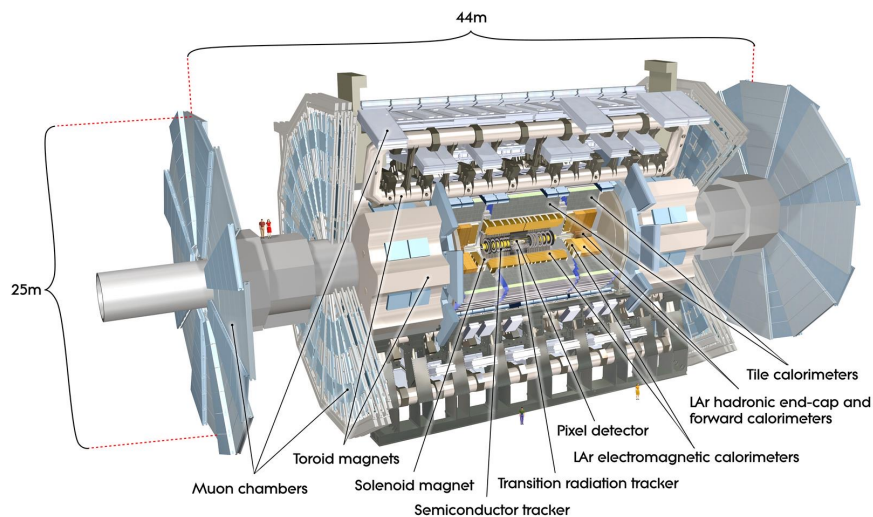
e.g. Baryon Number Transport



- \bar{p}/p ratio must be close to 1 in central region
- Decreases at large $|y|$ (or $|\eta|$) due to baryon number +1 beam particles
- Baryon number transport over $\Delta y \rightarrow 5$ rapidity units from beam particle

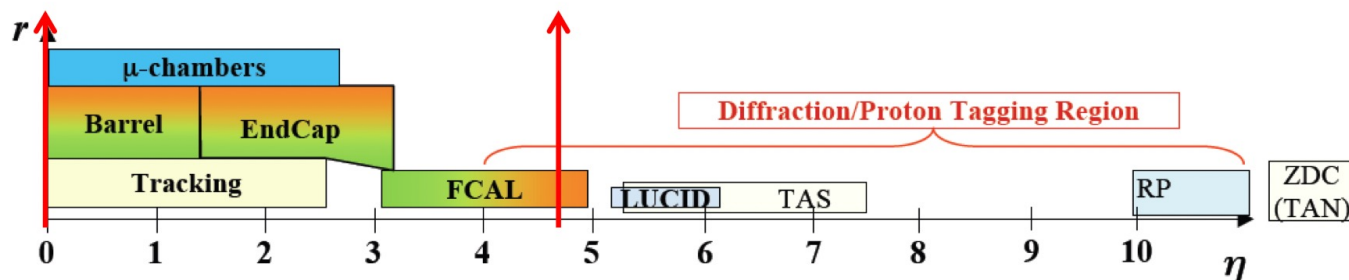
Rapidity Coverage at LHC

- System with centre of mass energy \sqrt{s} hadronises over (pseudo)-rapidity region $\Delta y \sim \ln \frac{s}{m_p^2}$ with roughly constant particle production per unit (pseudo)-rapidity in the central region, tailing off towards the beam particles
- Forward (large $|y|$) region in principle sensitive to low x physics, parton cascade dynamics and underlying event



- Main LHC experiments are focused on central region, but there is also forward instrumentation ...

- ‘Central’ ATLAS and CMS give information up to $|y| \sim 4.5 - 5.0$

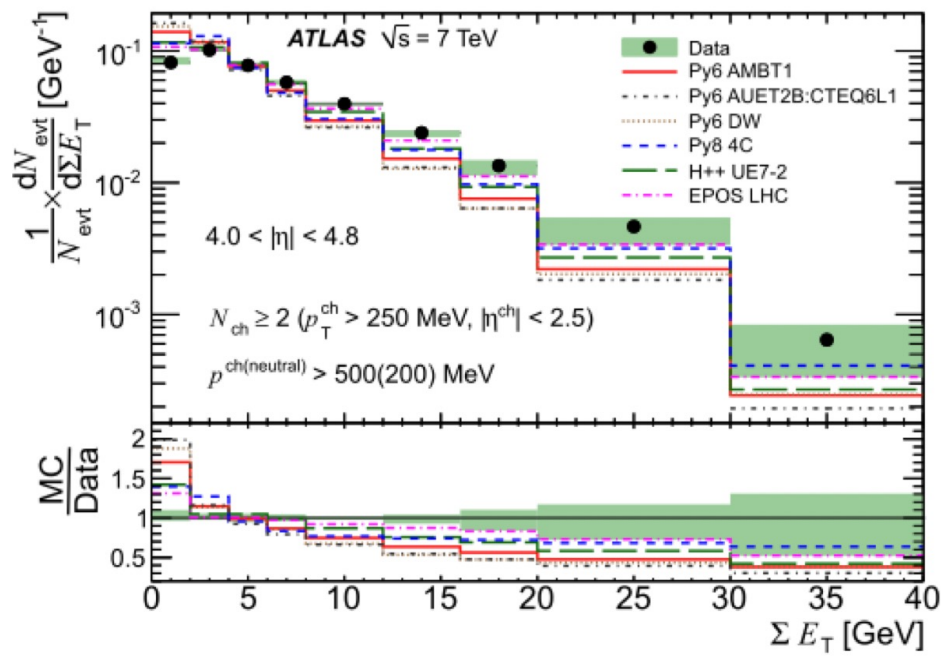
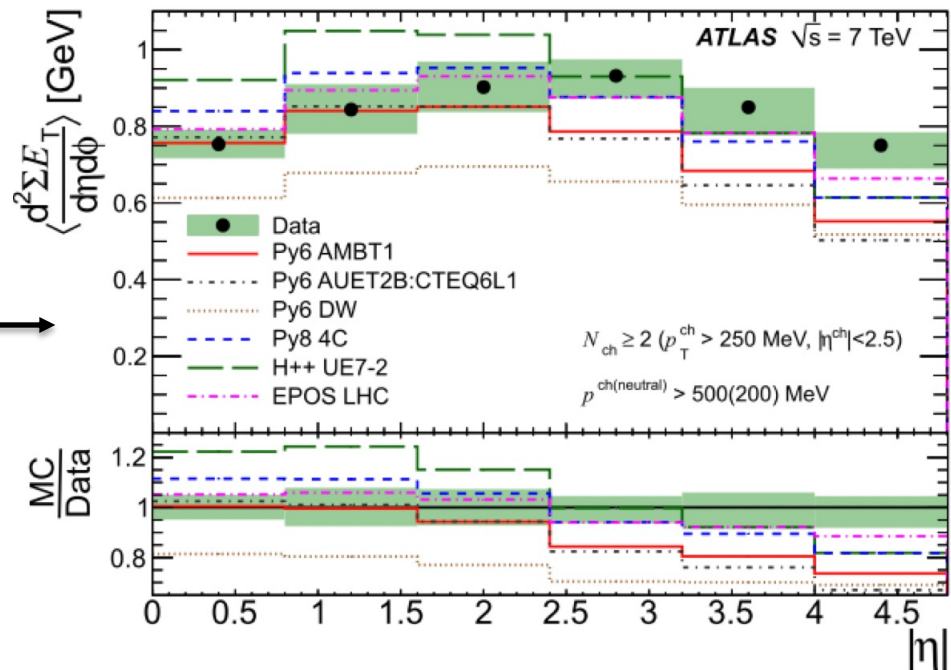
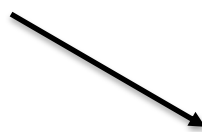


Example Data from main Detectors

Transverse Energy Flow versus $|\eta|$ up to $|\eta| = 4.8$)

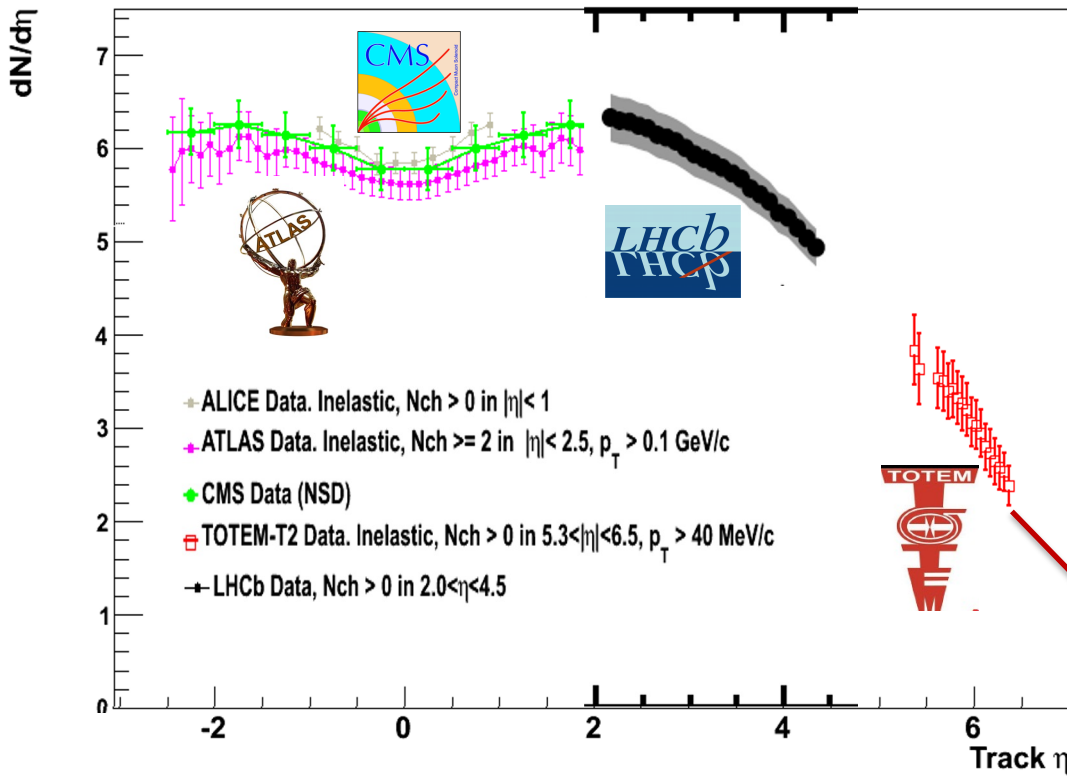
Total transverse energy with $4.0 < |\eta| < 4.8$

- No Monte Carlo models describe all features 'out of the box'
- Testing ground for models (mainly a tuning exercise) as used in eg cosmic ray air showers
- Complicated (rich!) physics, but hard to extract information about underlying QCD dynamics

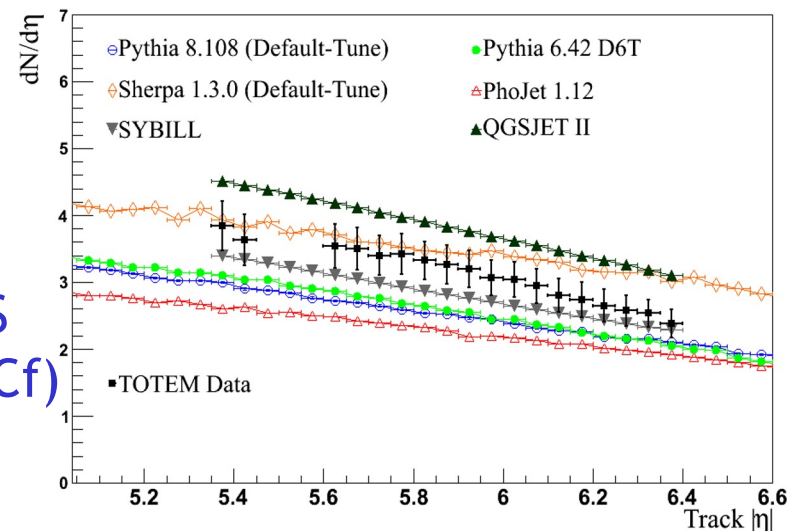


The Really Very Forward Region

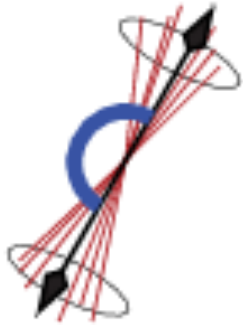
Charged particle multiplicity measurements beyond the rapidity plateau



- Very Forward tracking provided by LHCb and TOTEM T2 telescope ($5.3 < |\eta| < 6.5$) show changed behaviour towards beam
- Similarly calorimeters: ATLAS LUCID, CMS CASTOR and dedicated fwd experiments (LHCf)
- More for model tuning than deep insights



Dedicated low-x observables in LHC Physics

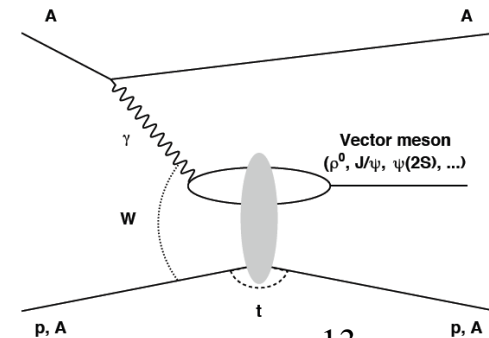
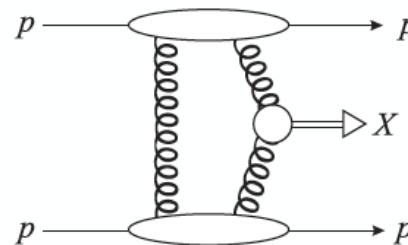
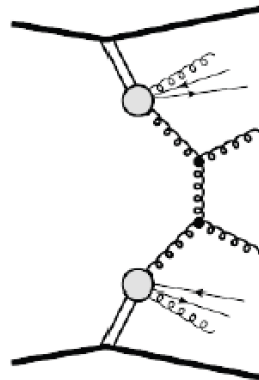
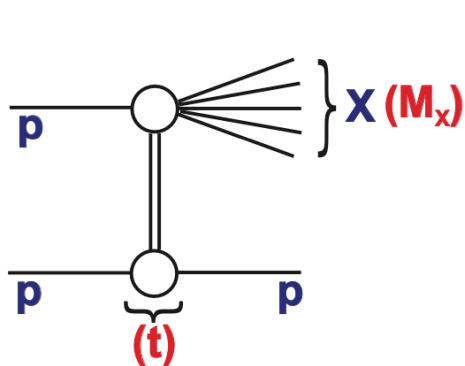
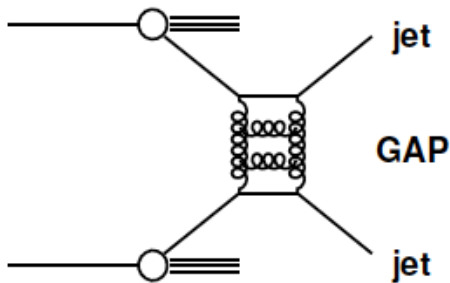


Example observables from early LHC studies:

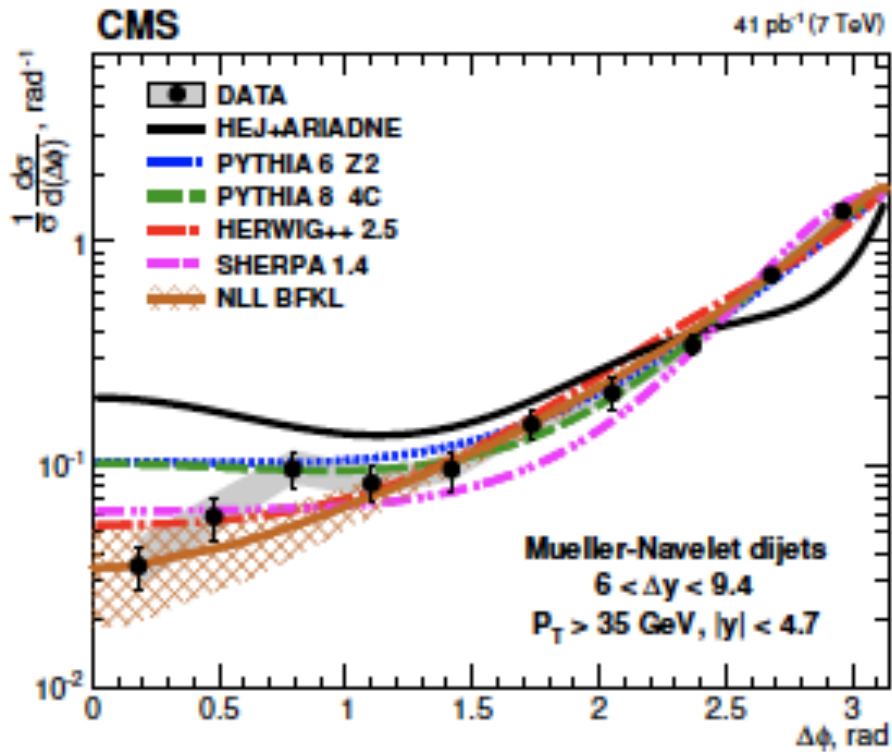
- Azimuthal decorrelations between jets
- Gaps between jets
- ...

Strongly interacting colour-singlet exchanges

- Elastic scattering (later today)
- Diffractive dissociation (later today)
- Central inclusive production (elsewhere)
- Central exclusive production (elsewhere)
- Ultra-peripheral collisions (next lecture)

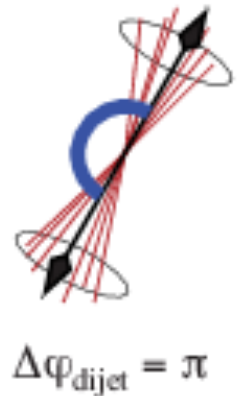


Azimuthal Decorrelations between Mueller-Navelet jets



- Choice of Forward-Backward highest E_T jets with comparable energy suppresses phase-space for DGLAP evolution and offers chance to search for BFKL evolution

- Sensitivity enhanced at large azimuthal decorrelation due to multiple emissions



... Jets separated by up to $\Delta y = 9.4$ units!

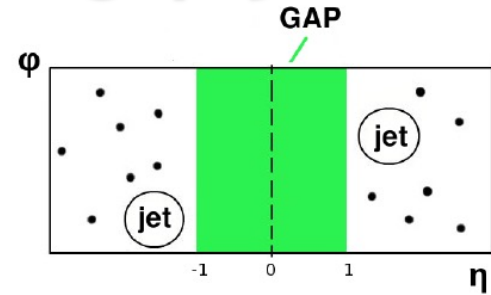
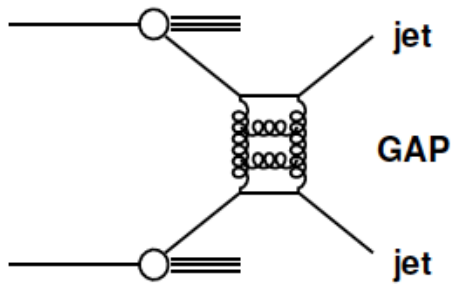
- LL BFKL model (HEJ) overestimates decorrelations
- Analytic NLL BFKL calculation agrees well with data

BUT

- DGLAP-based models with tuning also describe data

→ This is typical despite increasingly sophisticated observables

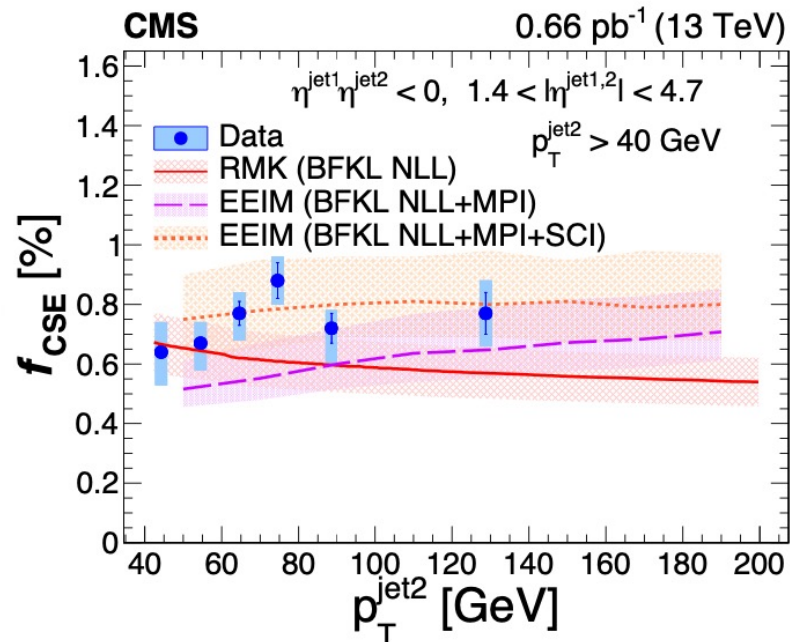
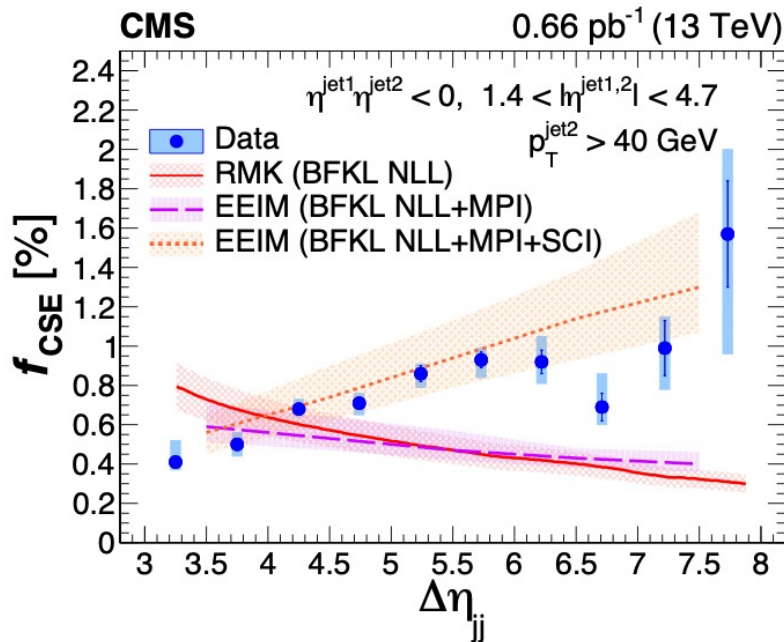
LHC Searches for BFKL Pomeron: Jet-gap-jet events



- Gaps between jets are classic signature for BFKL dynamics ('BFKL pomeron exchange')

- Complicated by rapidity gap survival / infrared safety and pile-up

- **Typical observable: fraction f_{CSE} of dijet events with gap versus size of gap**

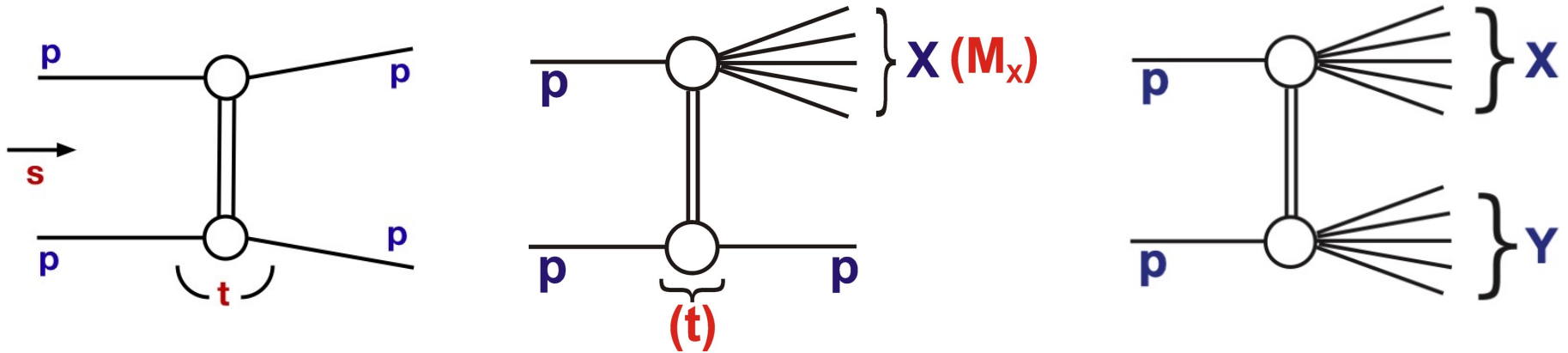


- Not describable with standard MC. Broad agreement with BFKL models.

Elastic and Diffractive Processes in Proton-Proton Collisions

[See also Valery Khoze lectures on 'High Energy soft QCD & Diffraction']

We are concerned with processes where no net quantum numbers are exchanged and the protons either stay intact or 'dissociate'

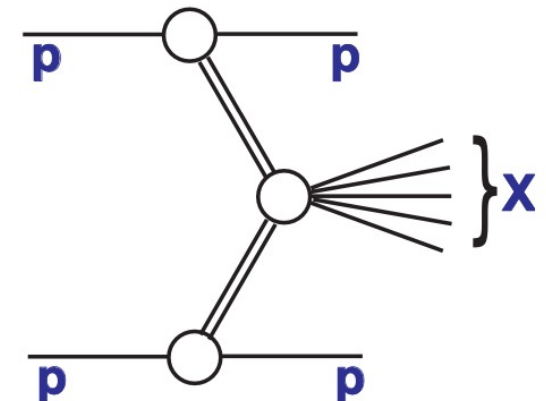


- There are also more complex topologies

- Experimental signatures:

... intact protons scattered through very small angles

... large regions with no particle production ('rapidity gaps')

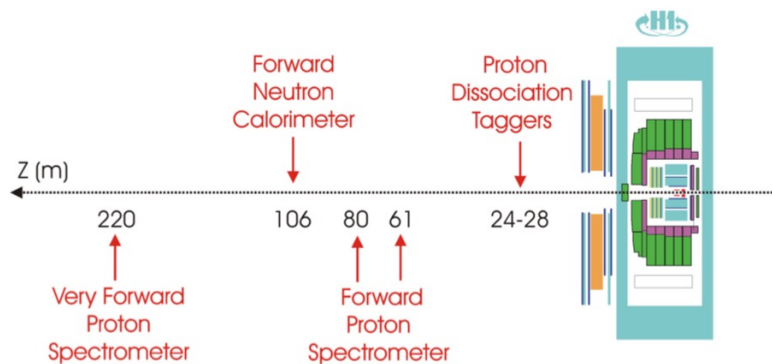


Methods for Diffraction and Elastic

... old slide from diffraction at HERA

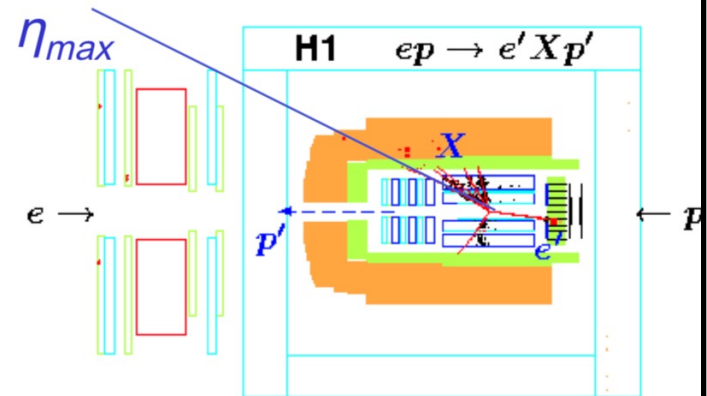
Signatures and Selection Methods

Scattered proton in Leading Proton Spectrometers (LPS)



Limited by statistics and p-tagging systematics

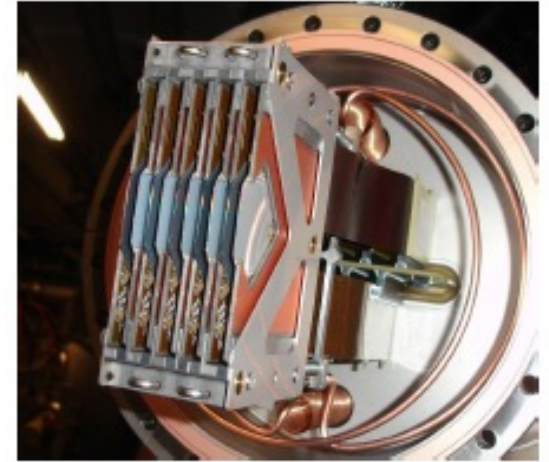
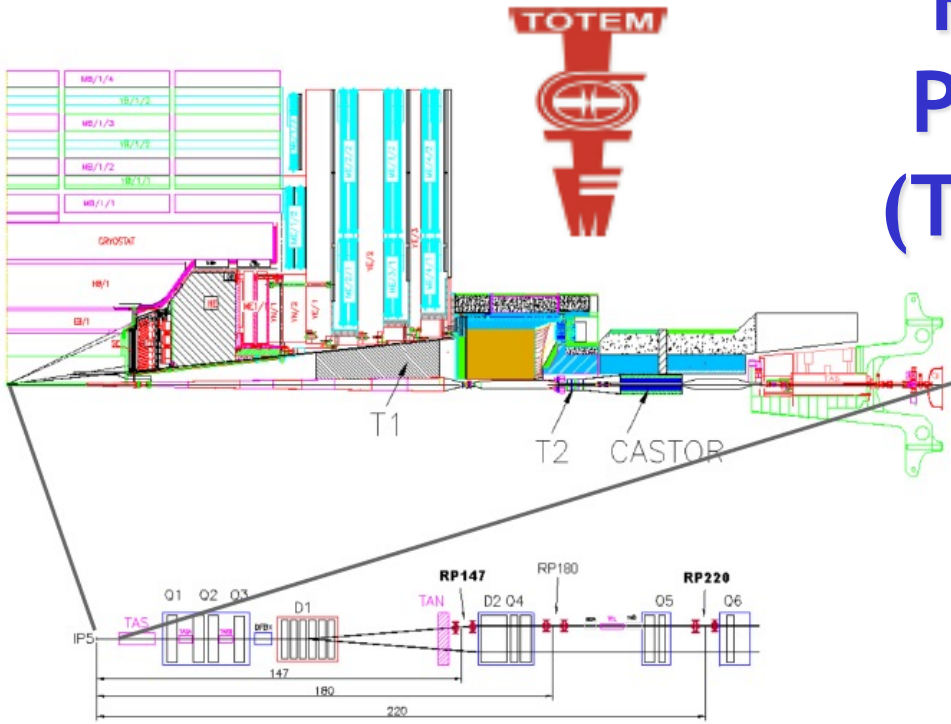
'Large Rapidity Gap' (LRG) adjacent to outgoing (untagged) proton



Limited by p-diss systematics

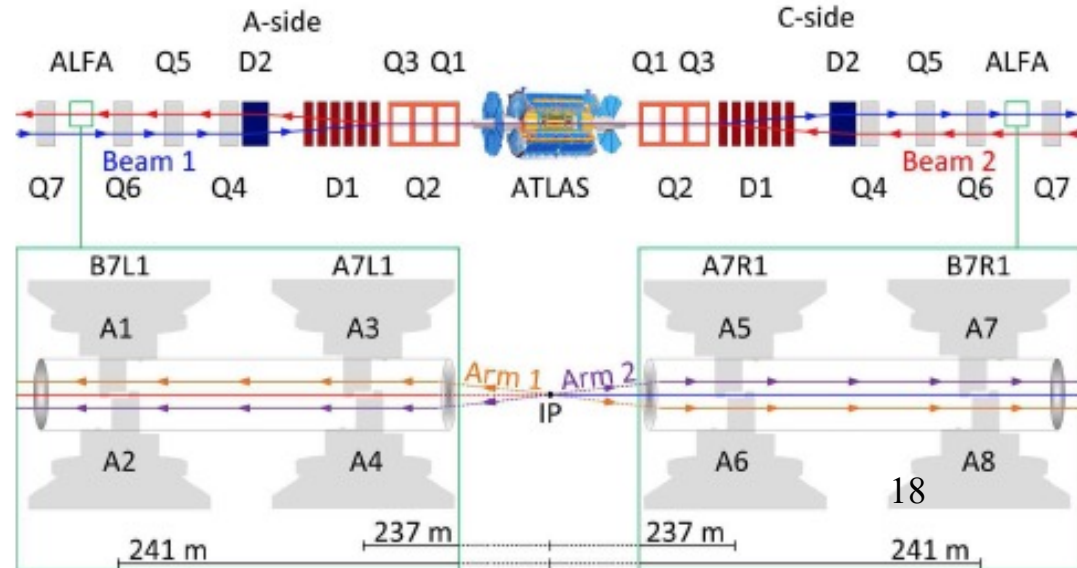
Partially still true for LHC (but proton tagging technology got better and rapidity gaps got harder to identify)

First Generation LHC Proton Spectrometers (TOTEM & ATLAS-ALFA)

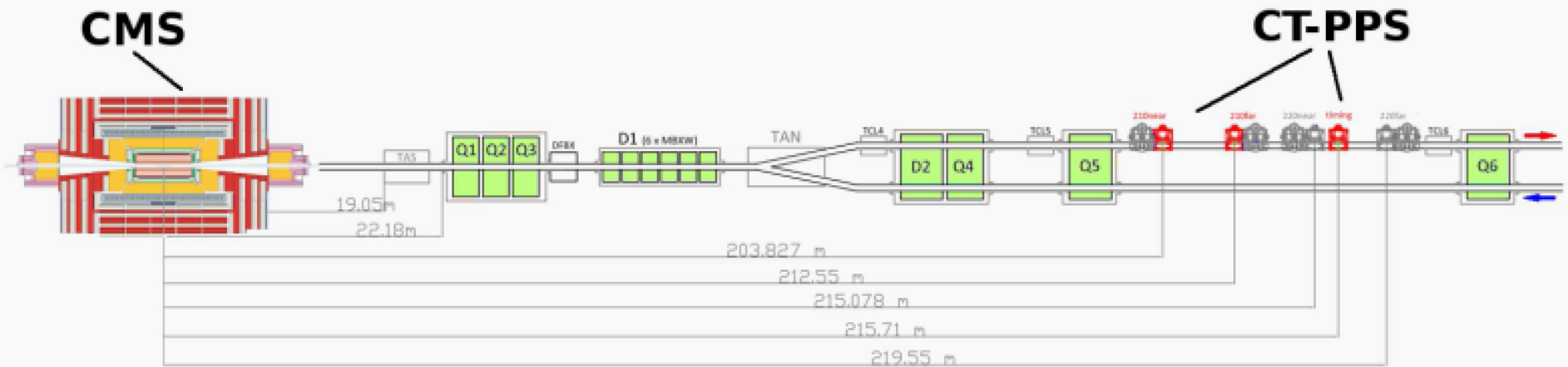


'Roman pot' vacuum-sealed insertions to beampipe, well downstream of IP.

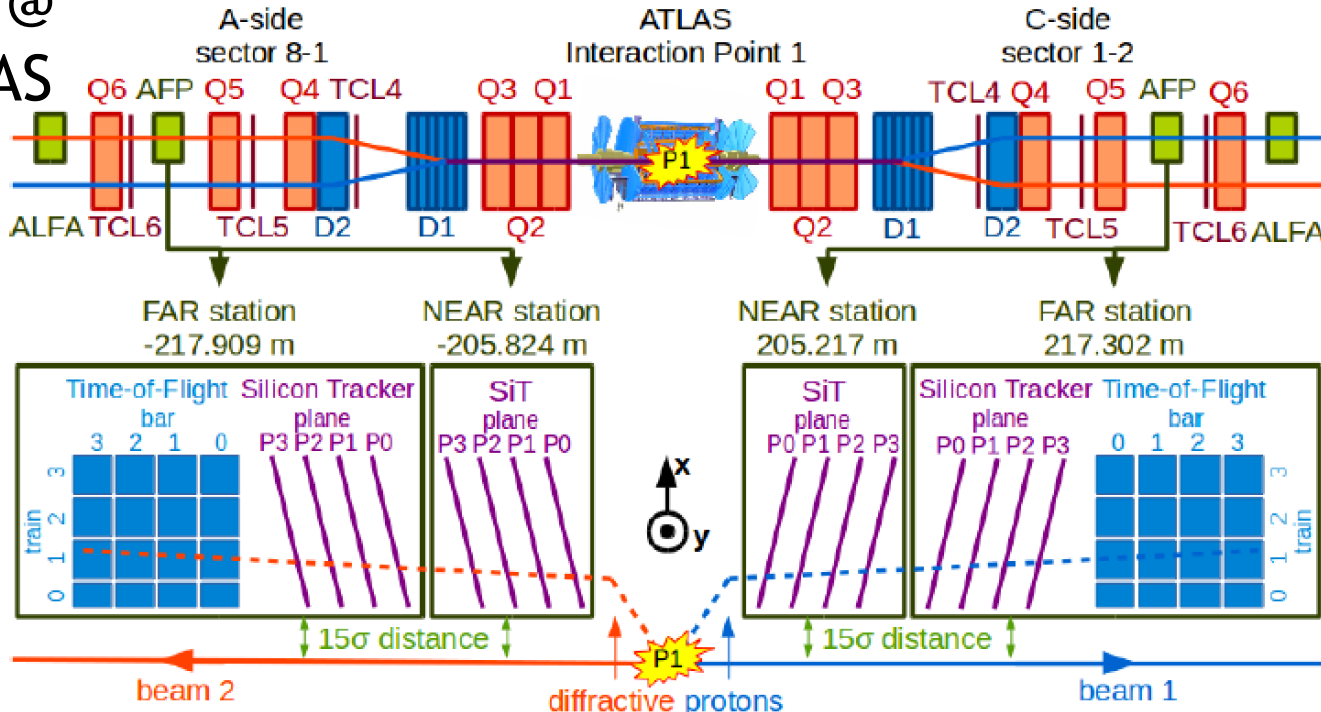
Not very radiation-hard
 → deployed in dedicated (high β^* , low luminosity) LHC runs



Second Generation LHC Proton Spectrometers (PPS at CMS and AFP at ALFA)



AFP @
ATLAS



Radiation-hard detectors, designed to operate in standard high luminosity running.

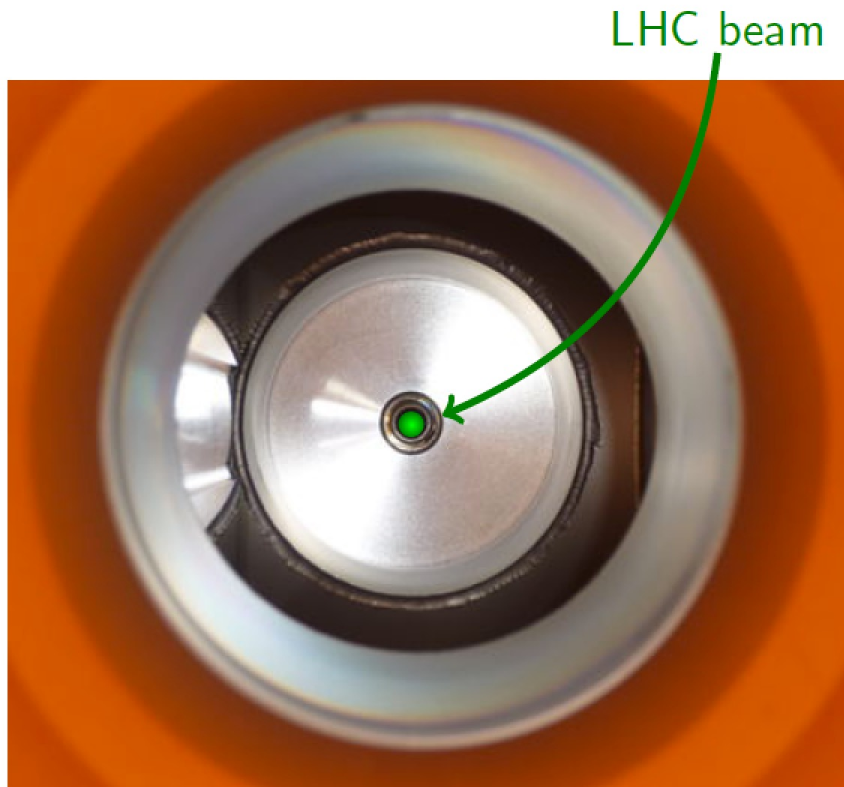
Principle of Roman Pot Detectors

Advantages of Roman Pot Technology



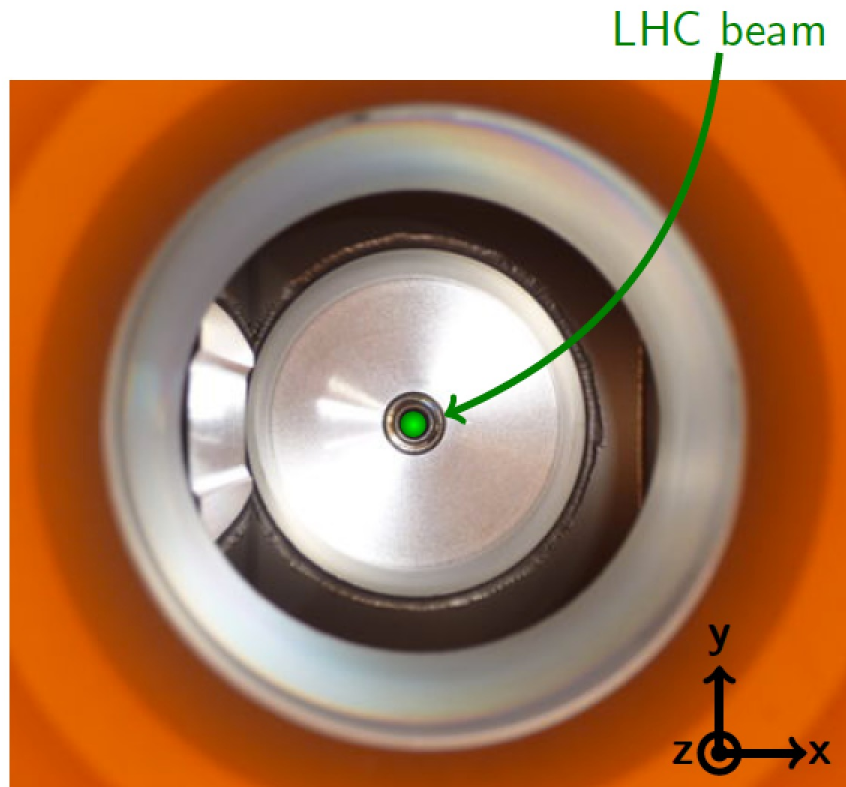
Principle of Roman Pot Detectors

Advantages of Roman Pot Technology



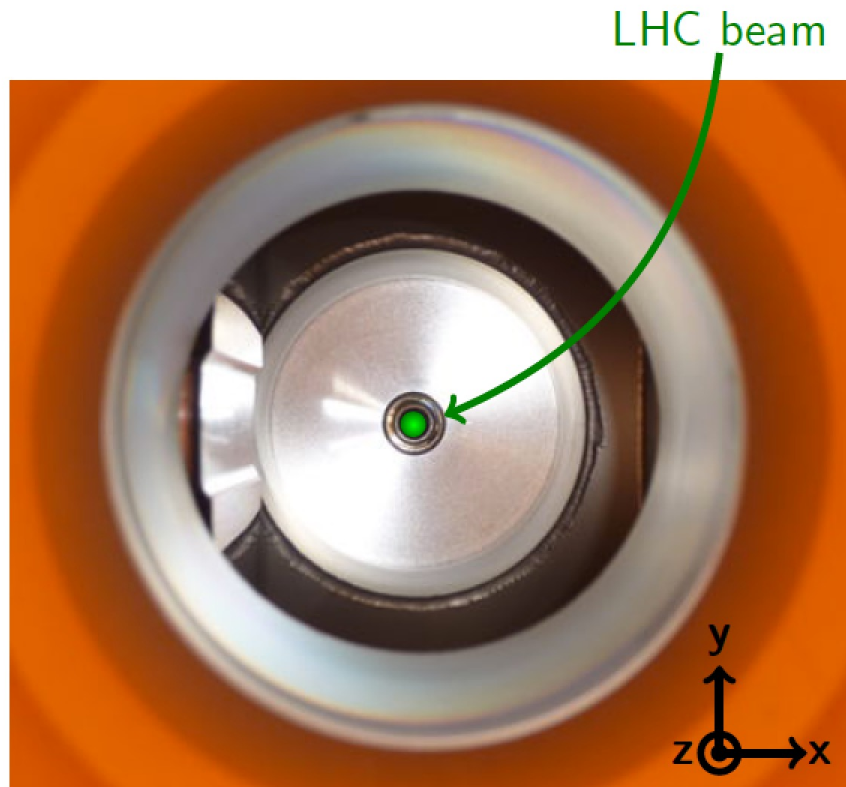
Principle of Roman Pot Detectors

Advantages of Roman Pot Technology



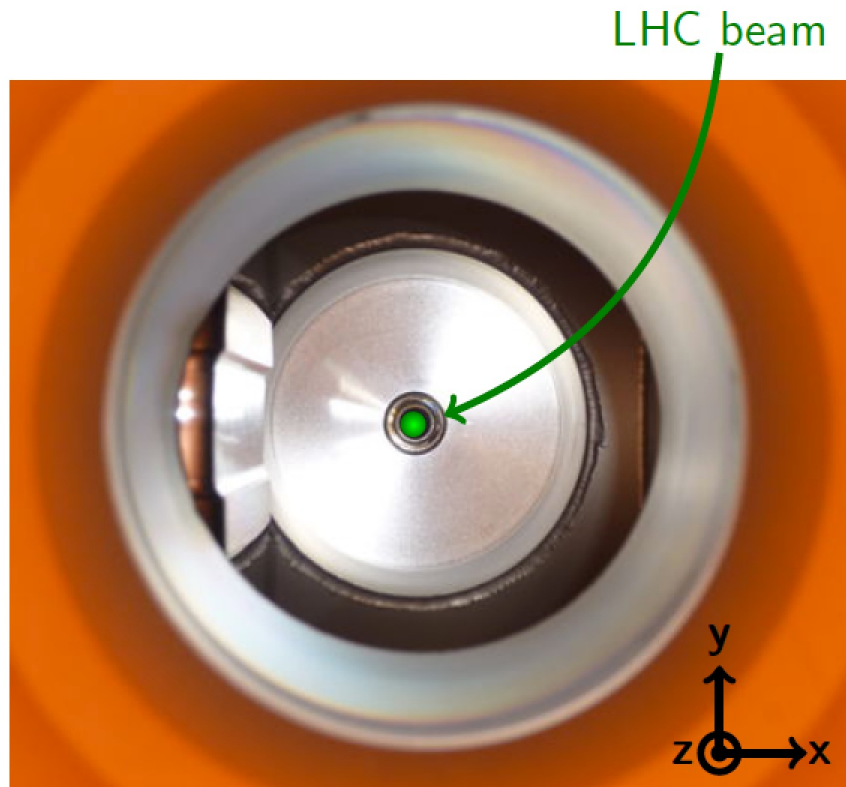
Principle of Roman Pot Detectors

Advantages of Roman Pot Technology



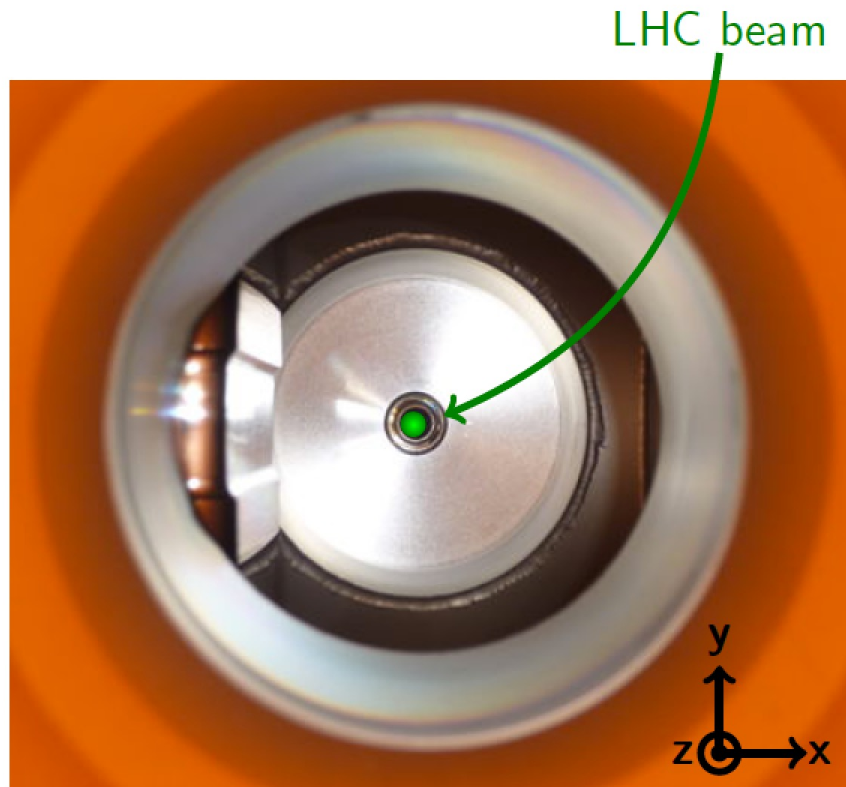
Principle of Roman Pot Detectors

Advantages of Roman Pot Technology



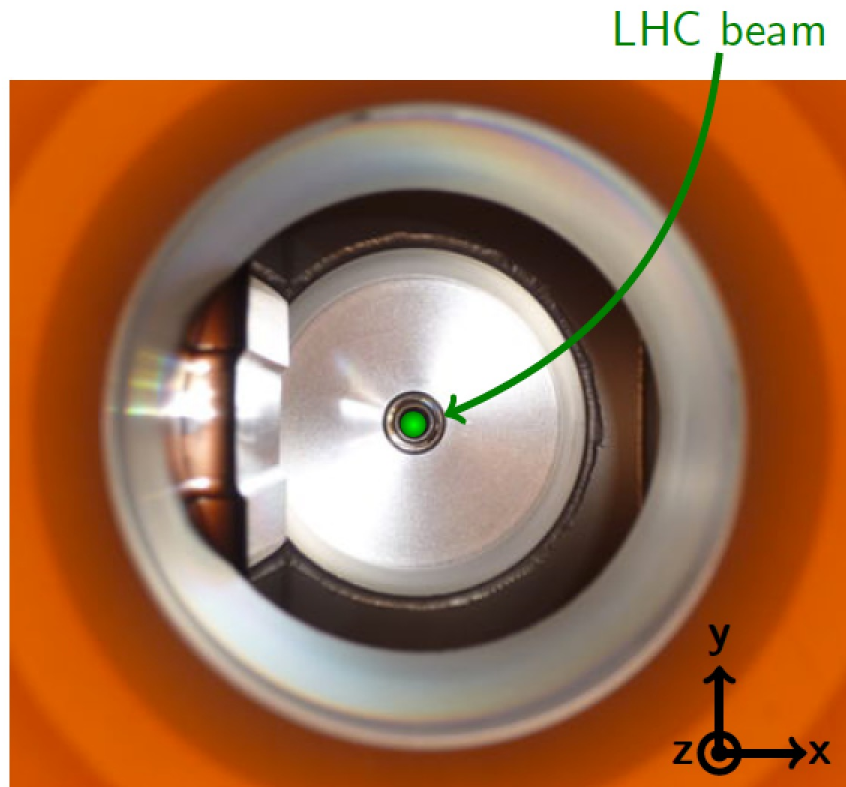
Principle of Roman Pot Detectors

Advantages of Roman Pot Technology



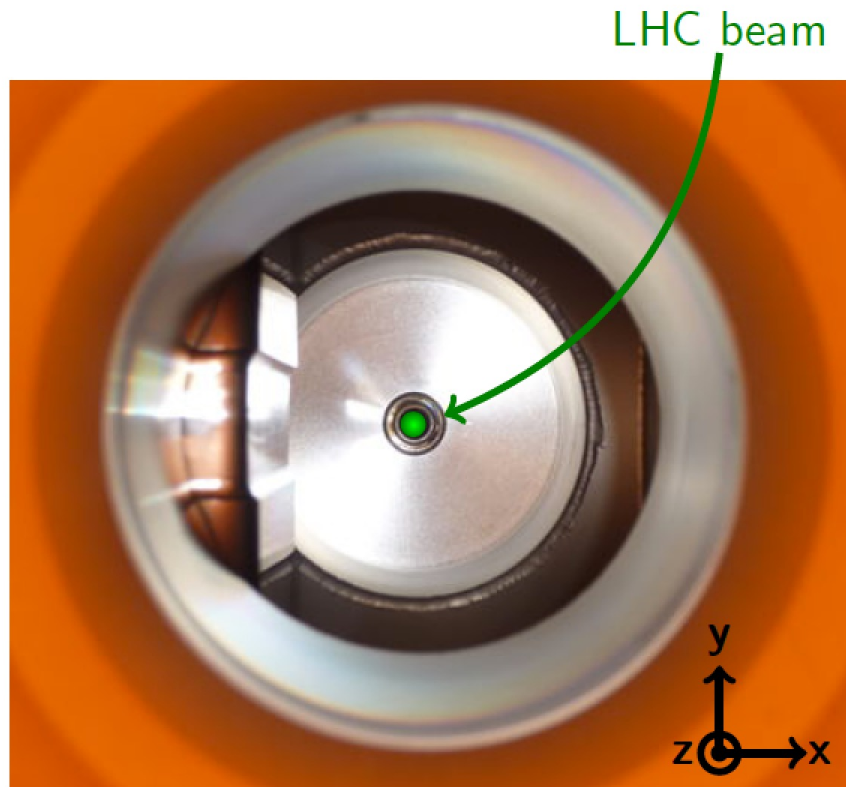
Principle of Roman Pot Detectors

Advantages of Roman Pot Technology



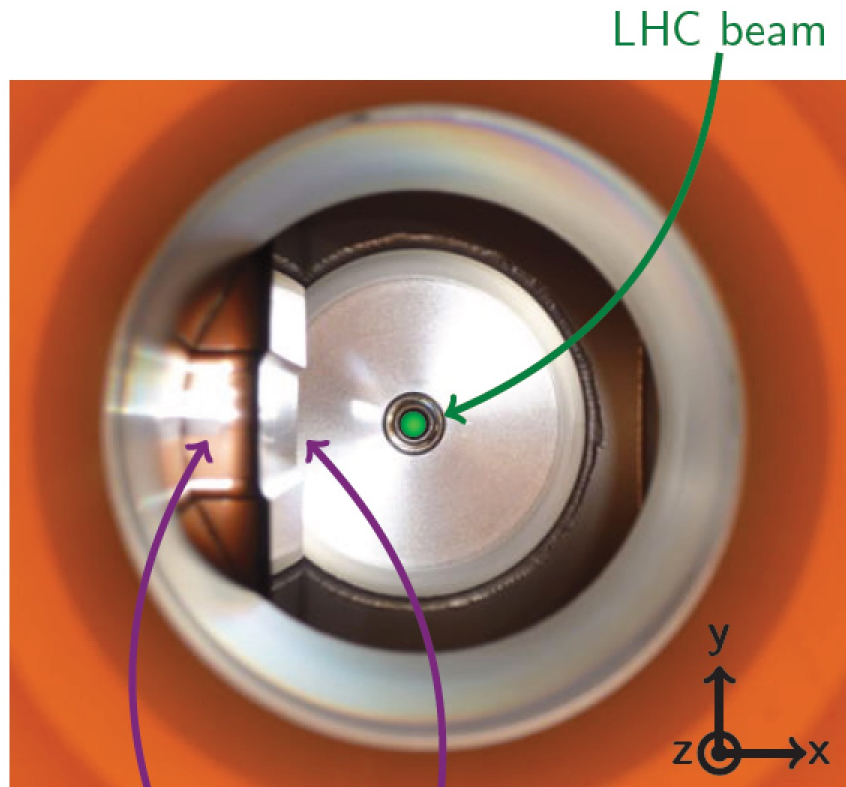
Principle of Roman Pot Detectors

Advantages of Roman Pot Technology



Principle of Roman Pot Detectors

Advantages of Roman Pot Technology

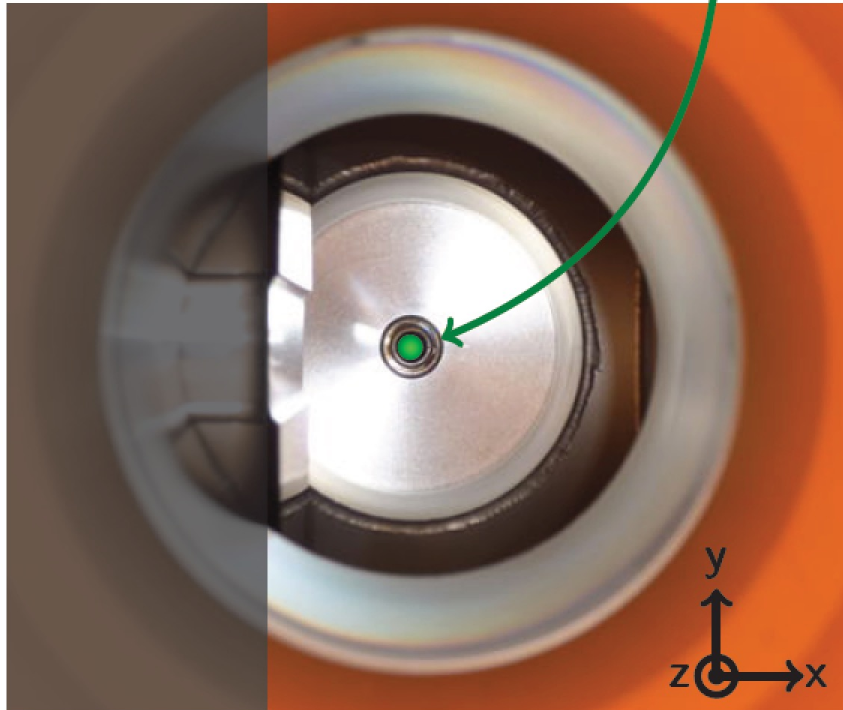


Principle of Roman Pot Detectors

Advantages of Roman Pot Technology

shadow of TCL4 and TCL5
collimators

LHC beam



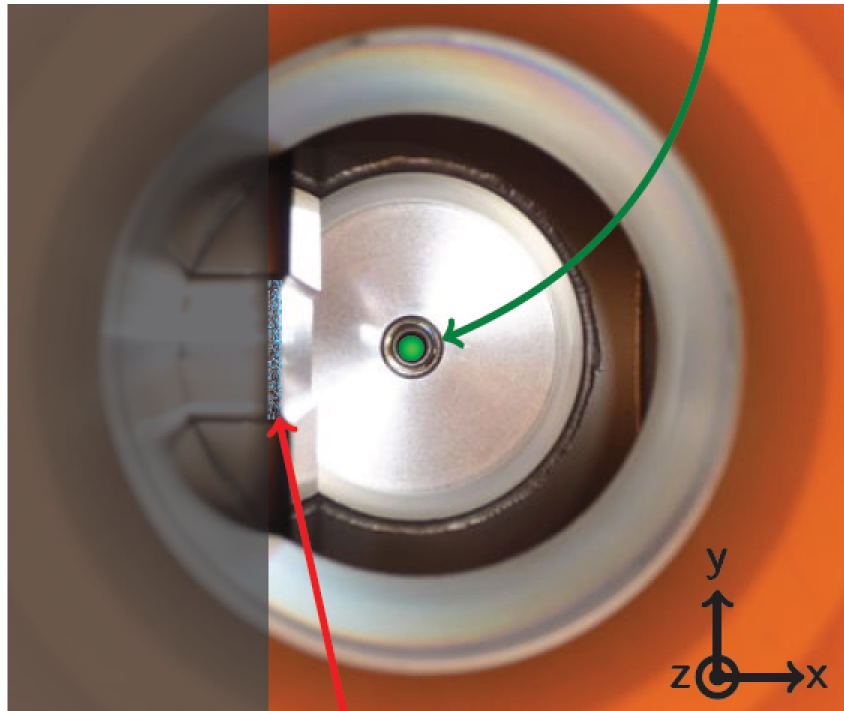
thin window and floor ($300 \mu\text{m}$)

Principle of Roman Pot Detectors

Advantages of Roman Pot Technology

shadow of TCL4 and TCL5 collimators

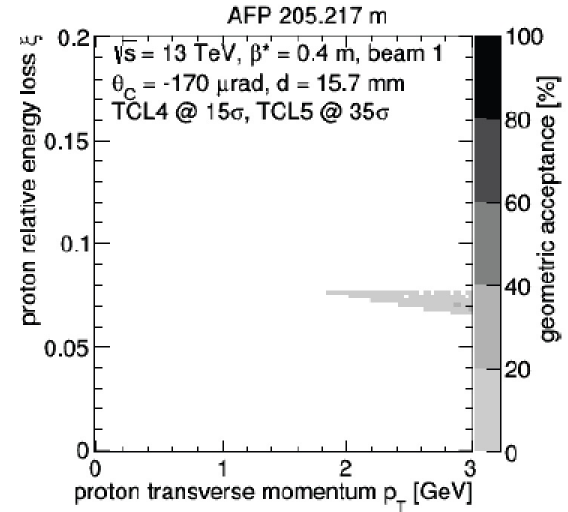
LHC beam



diffractive protons

thin window and floor ($300 \mu\text{m}$)

Geometric acceptance:

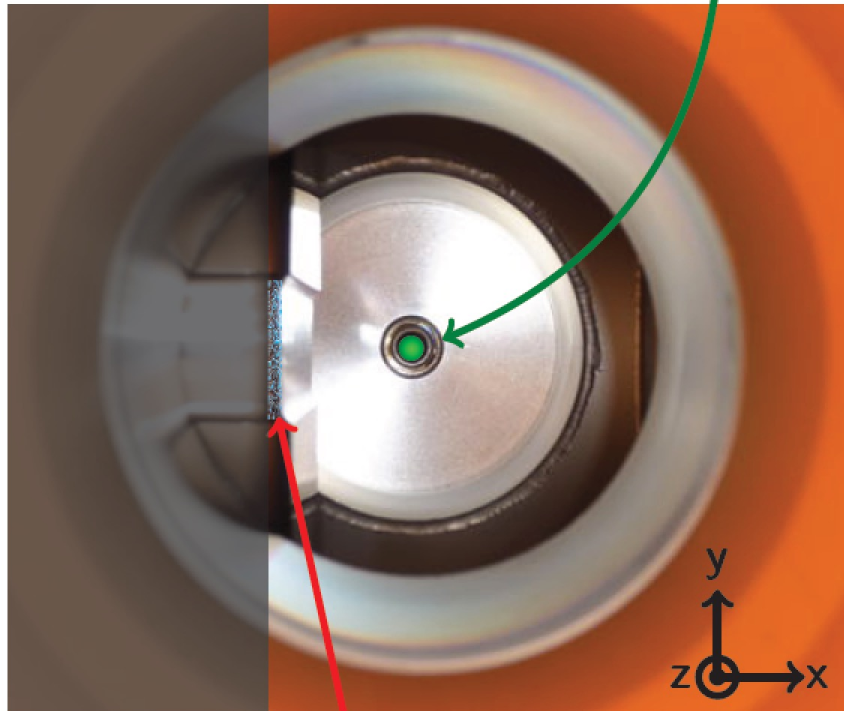


Principle of Roman Pot Detectors

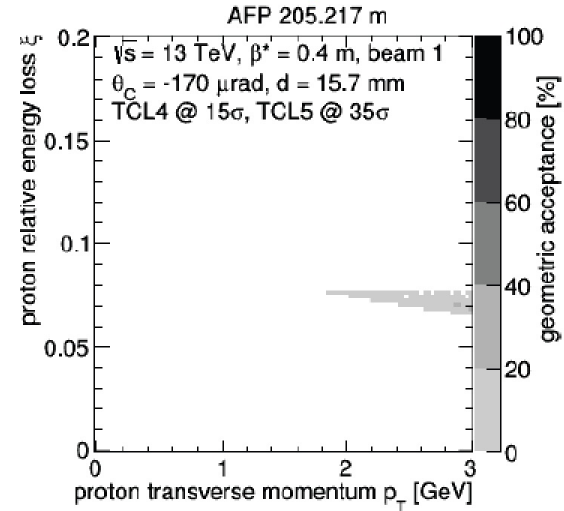
Advantages of Roman Pot Technology

shadow of TCL4 and TCL5 collimators

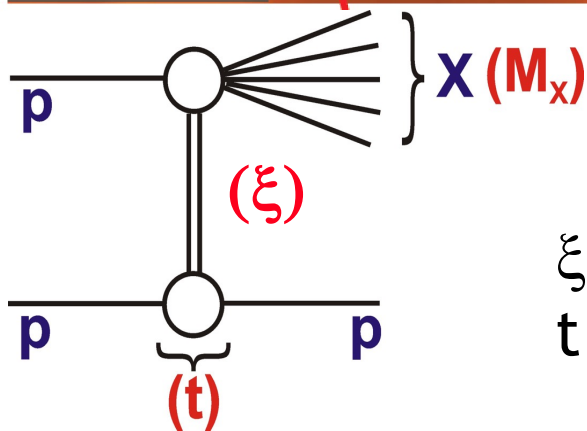
LHC beam



Geometric acceptance:



Described here in terms of kinematics of 'Single Diffractive Dissociation' (SD)



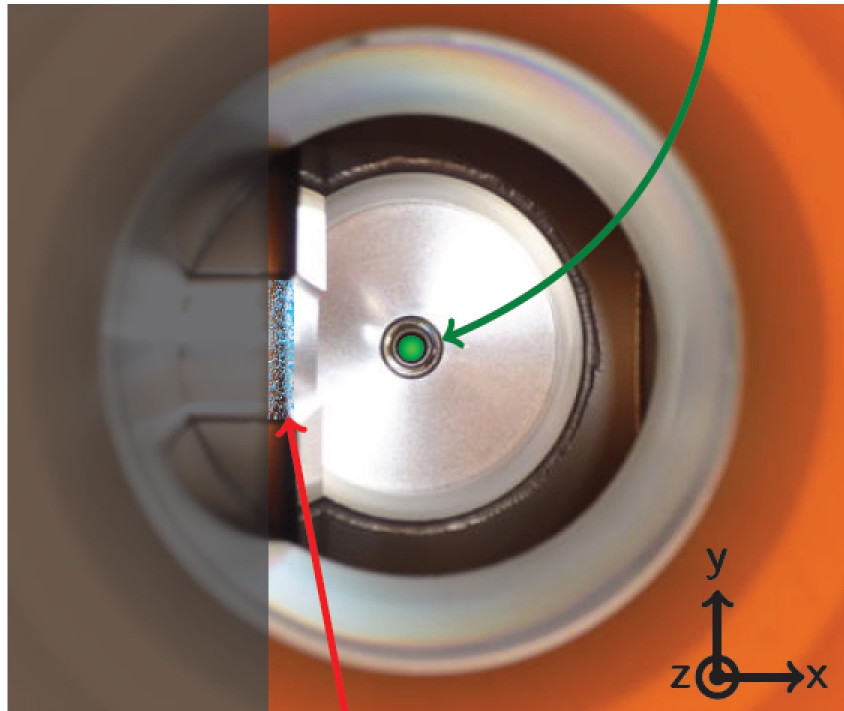
ξ = fractional proton energy loss
 $t = -p_T^2$ of outgoing proton

Principle of Roman Pot Detectors

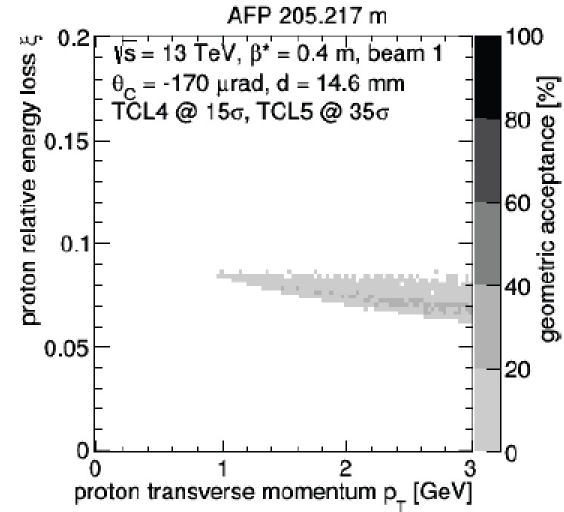
Advantages of Roman Pot Technology

shadow of TCL4 and TCL5 collimators

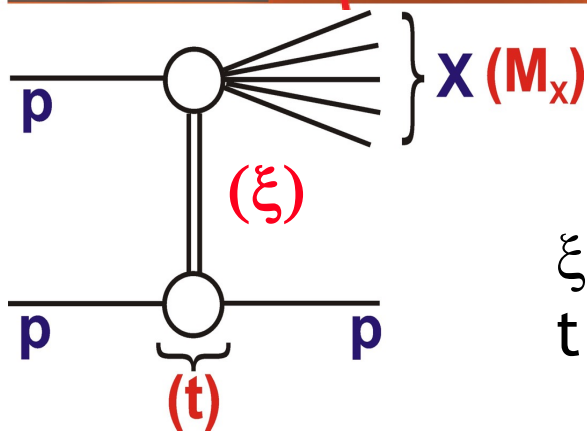
LHC beam



Geometric acceptance:



Described here in terms of kinematics of 'Single Diffractive Dissociation' (SD)



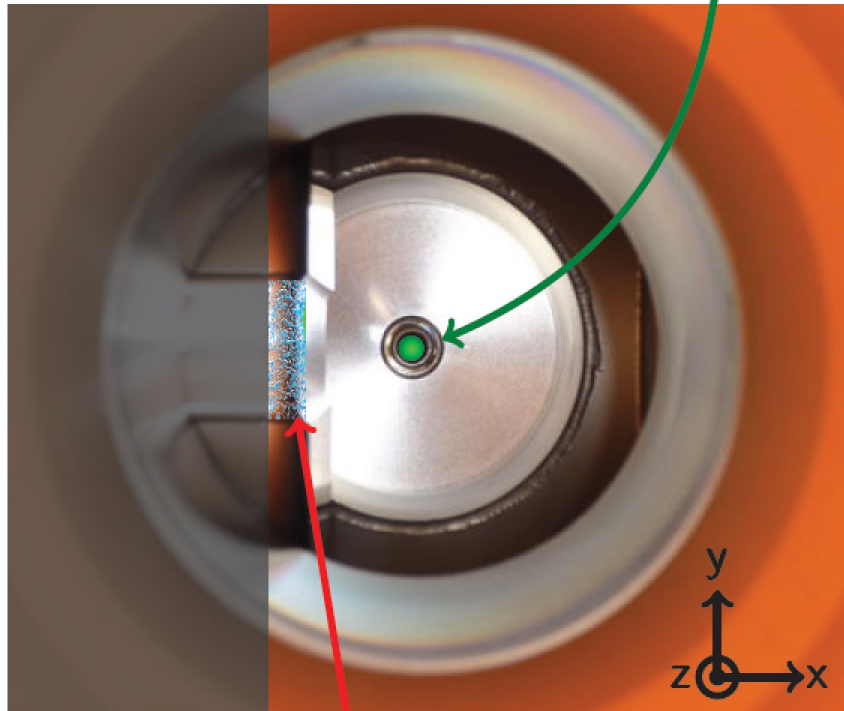
ξ = fractional proton energy loss
 $t = -p_T^2$ of outgoing proton

Principle of Roman Pot Detectors

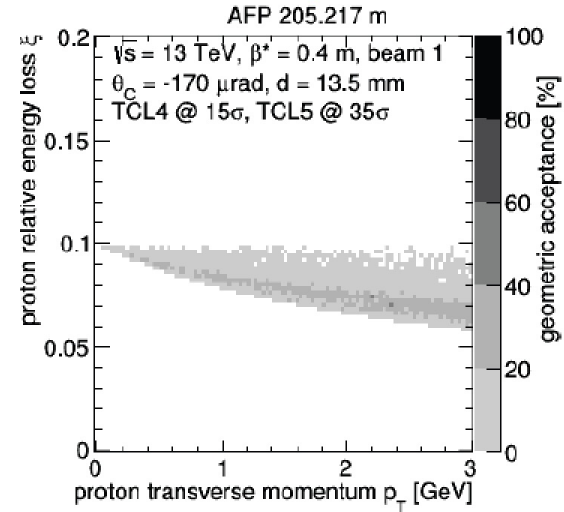
Advantages of Roman Pot Technology

shadow of TCL4 and TCL5 collimators

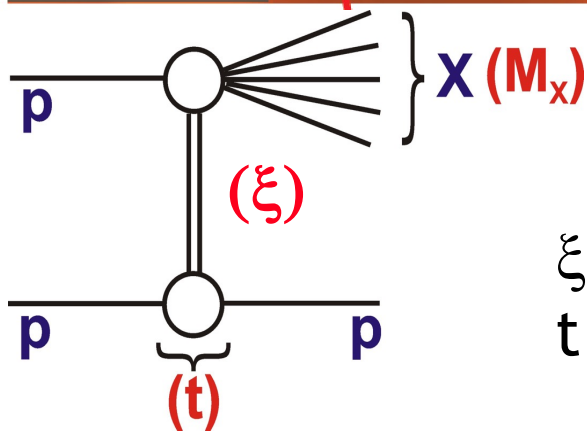
LHC beam



Geometric acceptance:



Described here in terms of kinematics of 'Single Diffractive Dissociation' (SD)



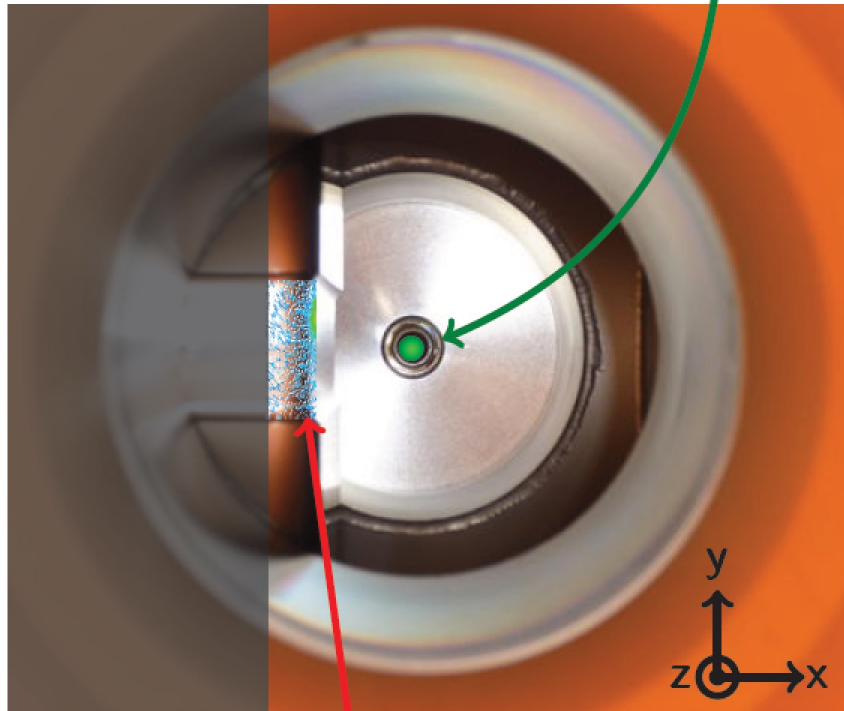
ξ = fractional proton energy loss
 $t = -p_T^2$ of outgoing proton

Principle of Roman Pot Detectors

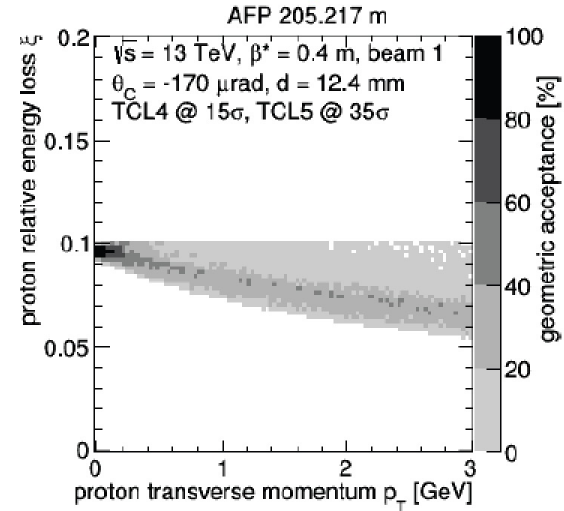
Advantages of Roman Pot Technology

shadow of TCL4 and TCL5 collimators

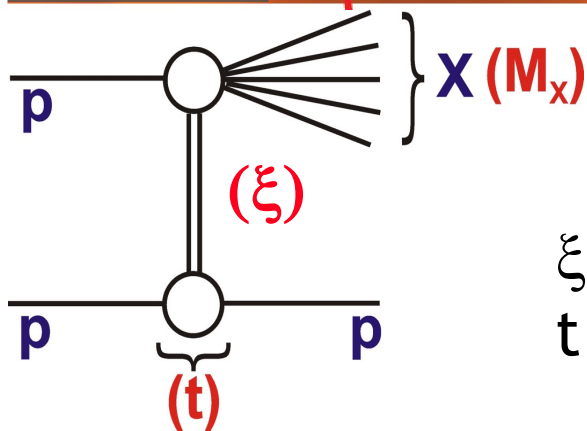
LHC beam



Geometric acceptance:



Described here in terms of kinematics of 'Single Diffractive Dissociation' (SD)



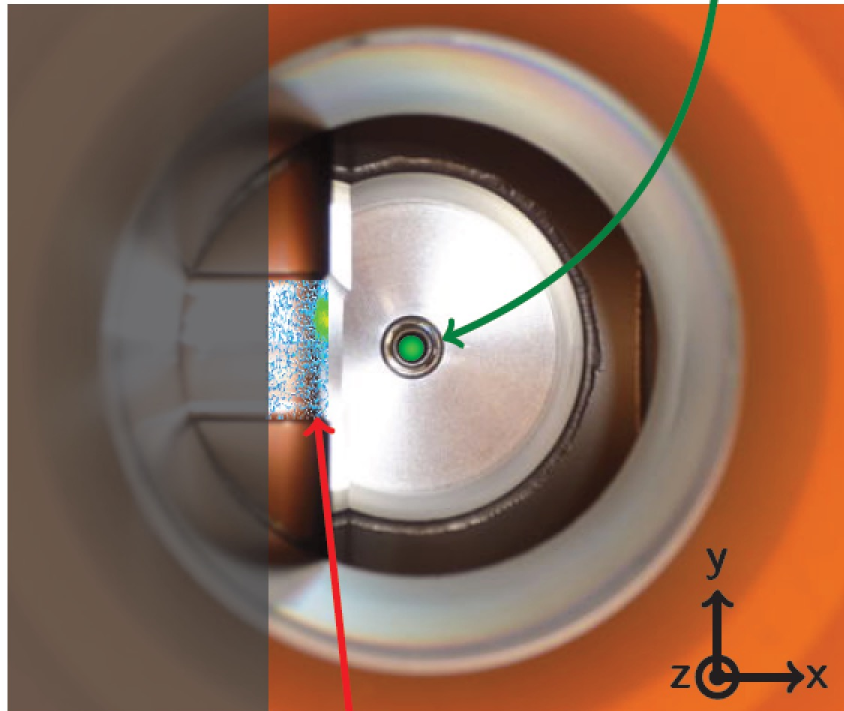
ξ = fractional proton energy loss
 $t = -p_T^2$ of outgoing proton

Principle of Roman Pot Detectors

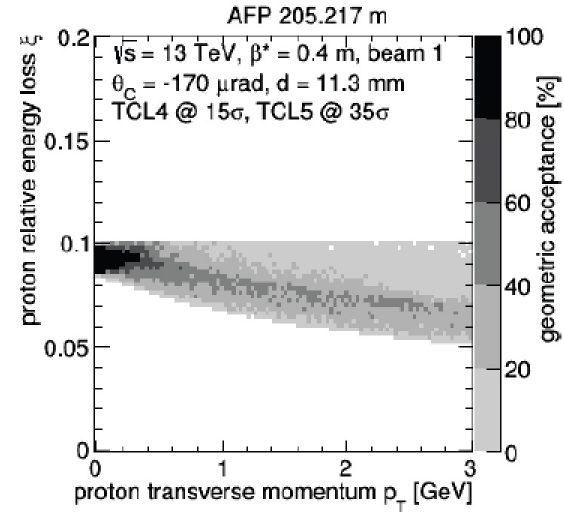
Advantages of Roman Pot Technology

shadow of TCL4 and TCL5 collimators

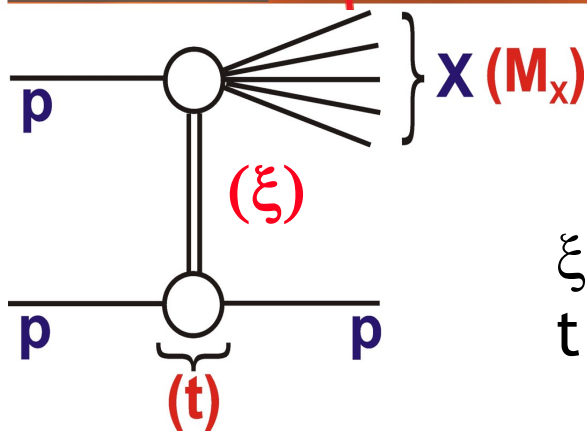
LHC beam



Geometric acceptance:



Described here in terms of kinematics of 'Single Diffractive Dissociation' (SD)



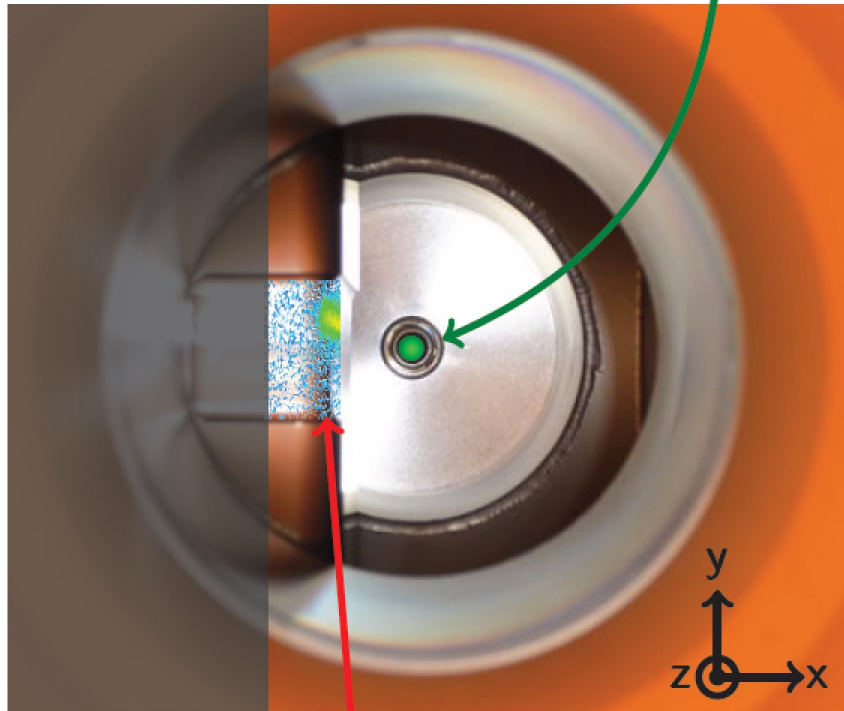
ξ = fractional proton energy loss
 $t = -p_T^2$ of outgoing proton

Principle of Roman Pot Detectors

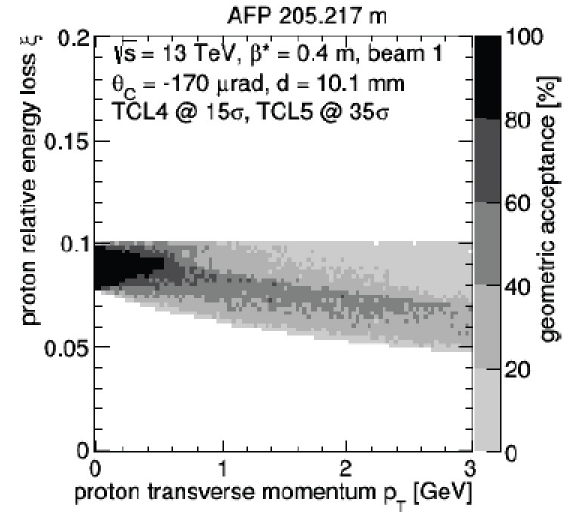
Advantages of Roman Pot Technology

shadow of TCL4 and TCL5 collimators

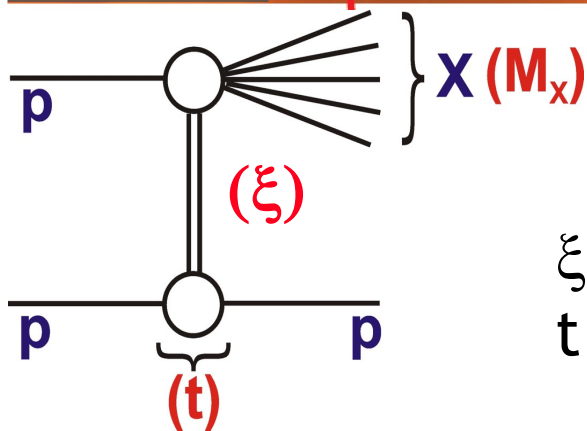
LHC beam



Geometric acceptance:



Described here in terms of kinematics of 'Single Diffractive Dissociation' (SD)



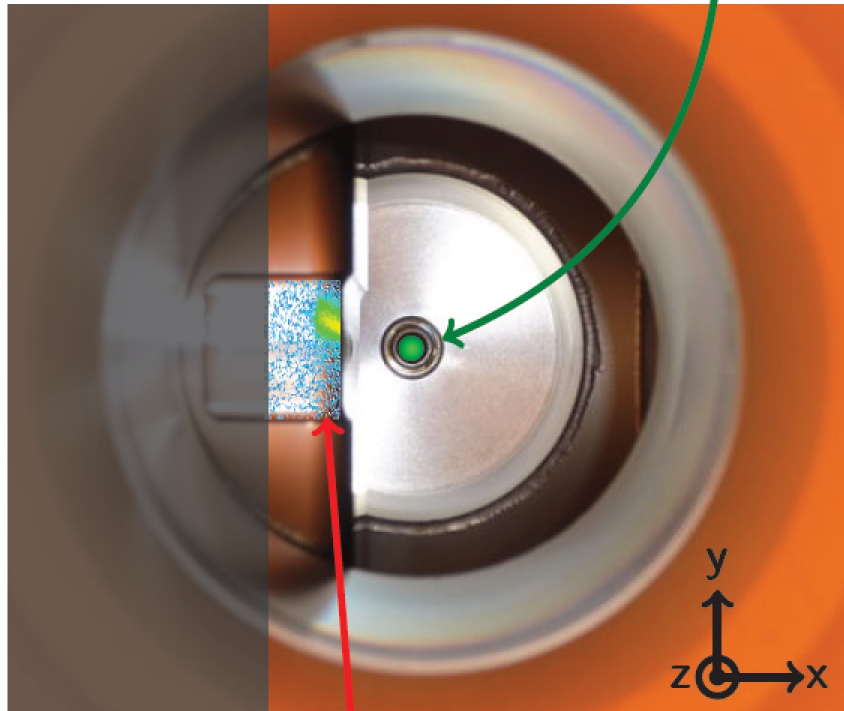
ξ = fractional proton energy loss
 $t = -p_T^2$ of outgoing proton

Principle of Roman Pot Detectors

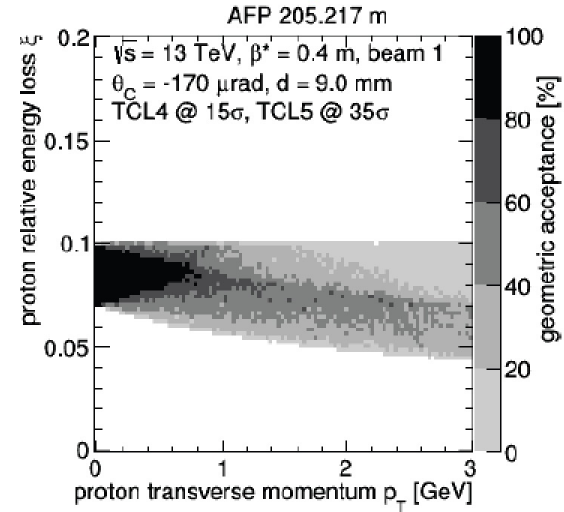
Advantages of Roman Pot Technology

shadow of TCL4 and TCL5 collimators

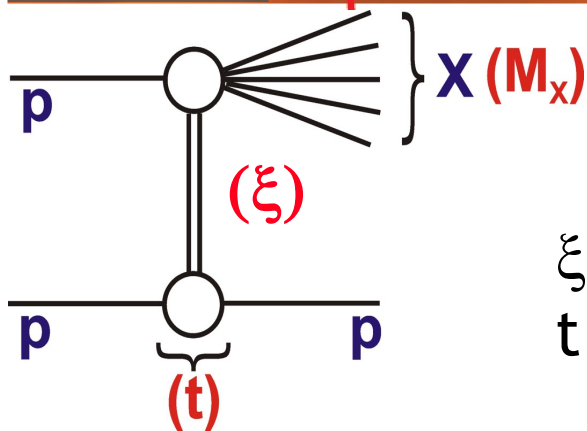
LHC beam



Geometric acceptance:



Described here in terms of kinematics of 'Single Diffractive Dissociation' (SD)



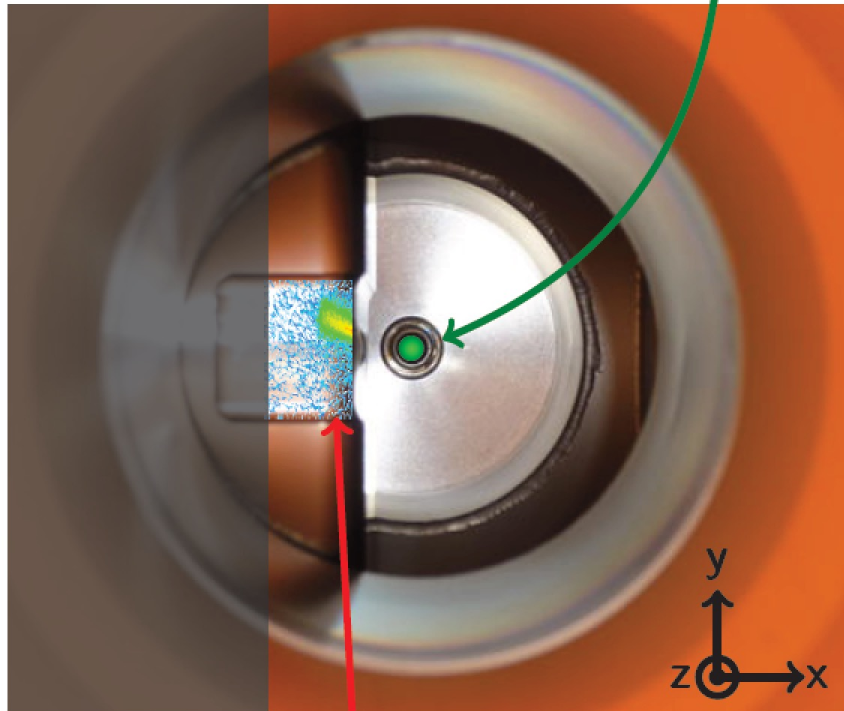
ξ = fractional proton energy loss
 $t = -p_T^2$ of outgoing proton

Principle of Roman Pot Detectors

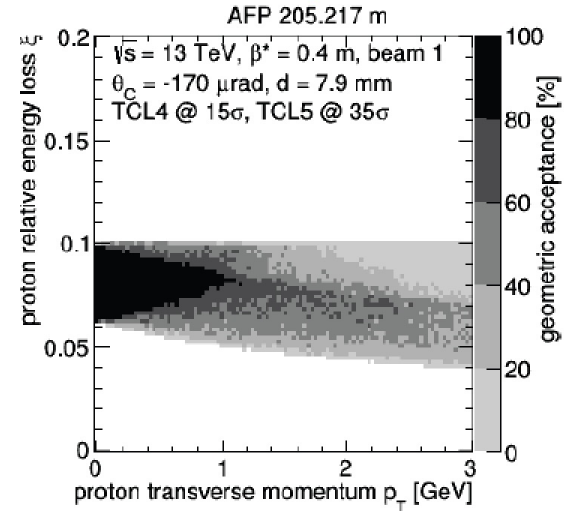
Advantages of Roman Pot Technology

shadow of TCL4 and TCL5 collimators

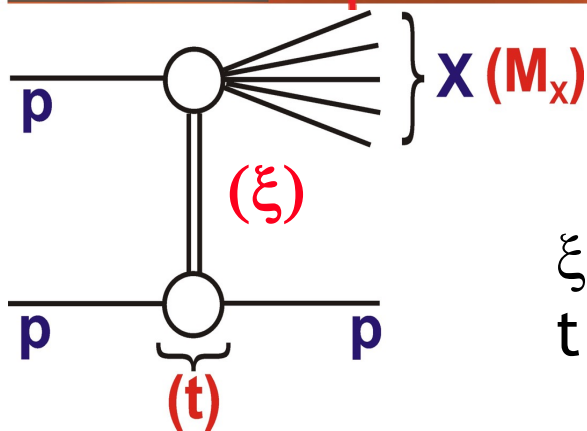
LHC beam



Geometric acceptance:



Described here in terms of kinematics of 'Single Diffractive Dissociation' (SD)



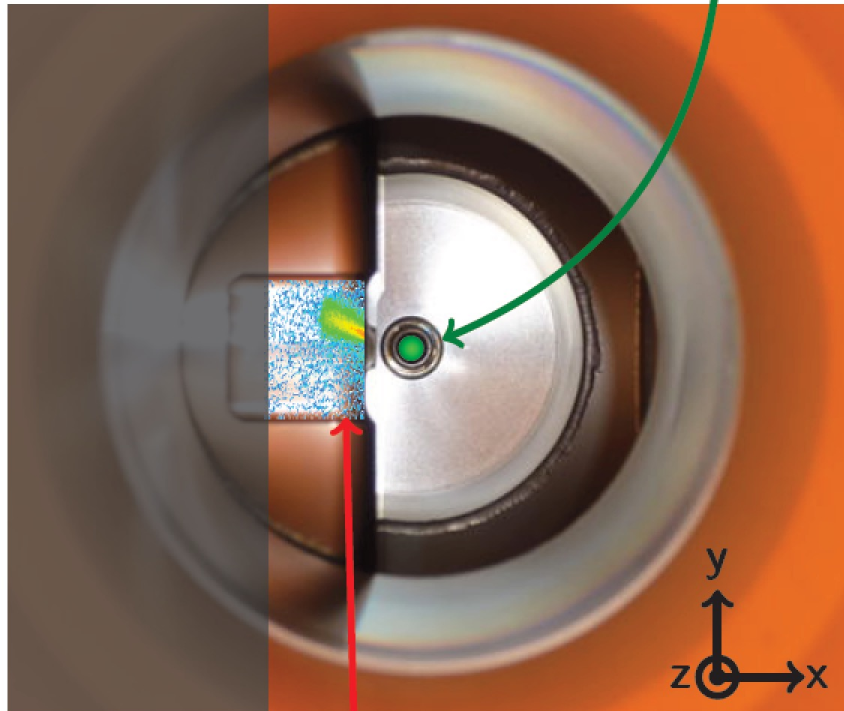
ξ = fractional proton energy loss
 $t = -p_T^2$ of outgoing proton

Principle of Roman Pot Detectors

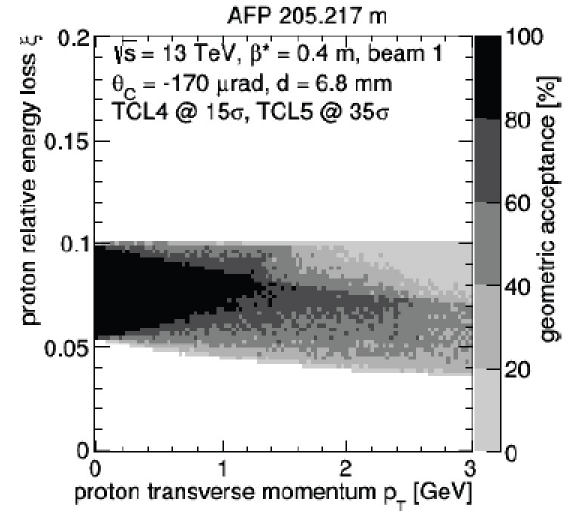
Advantages of Roman Pot Technology

shadow of TCL4 and TCL5 collimators

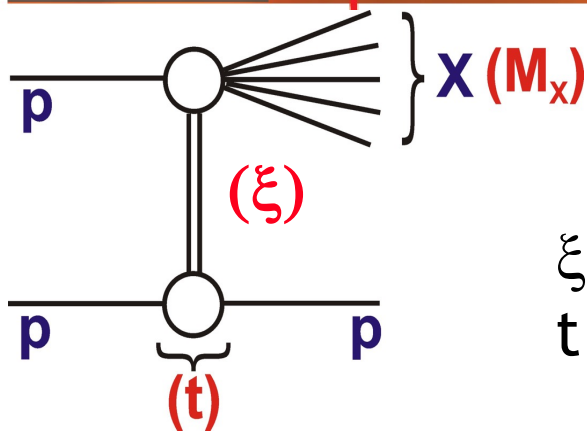
LHC beam



Geometric acceptance:



Described here in terms of kinematics of 'Single Diffractive Dissociation' (SD)



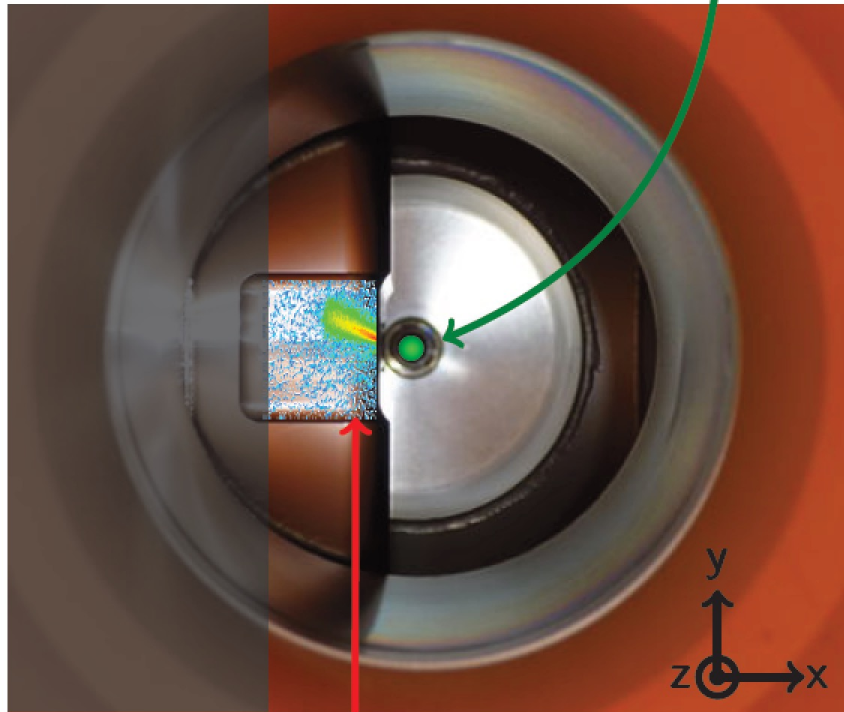
ξ = fractional proton energy loss
 $t = -p_T^2$ of outgoing proton

Principle of Roman Pot Detectors

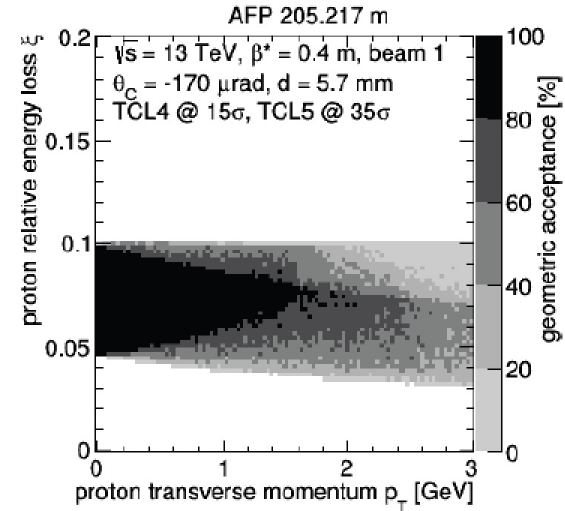
Advantages of Roman Pot Technology

shadow of TCL4 and TCL5 collimators

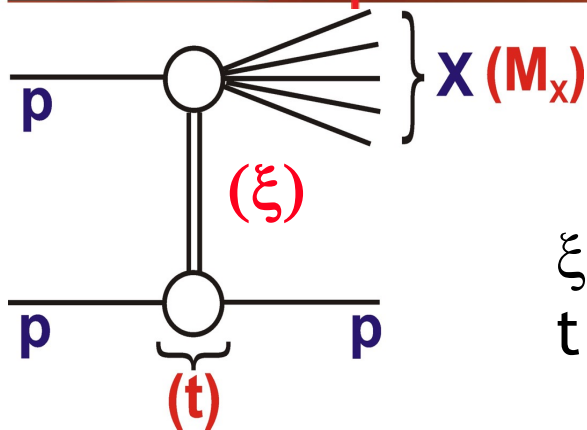
LHC beam



Geometric acceptance:



Described here in terms of kinematics of 'Single Diffractive Dissociation' (SD)



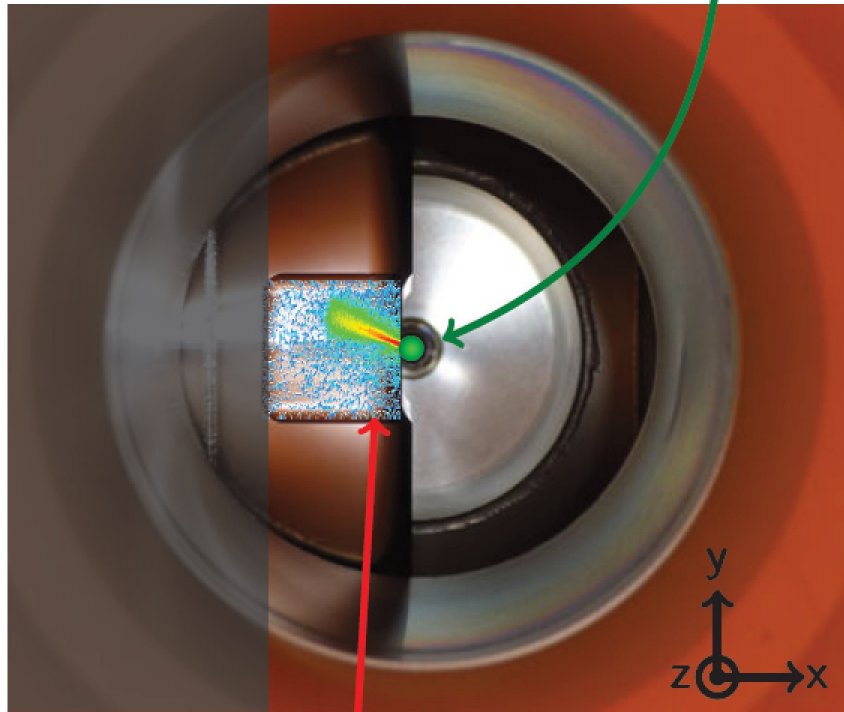
ξ = fractional proton energy loss
 $t = -p_T^2$ of outgoing proton

Principle of Roman Pot Detectors

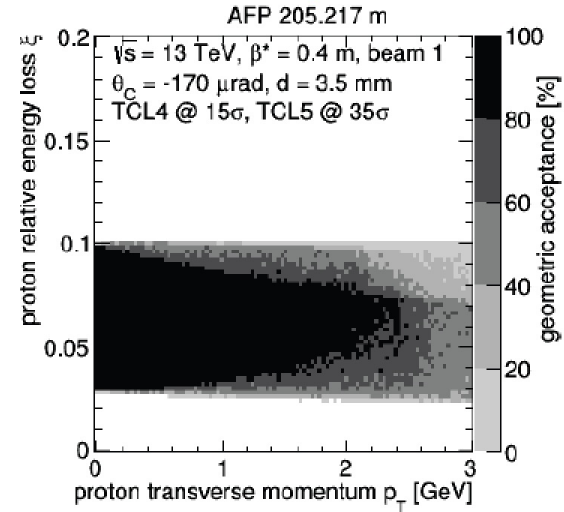
Advantages of Roman Pot Technology

shadow of TCL4 and TCL5 collimators

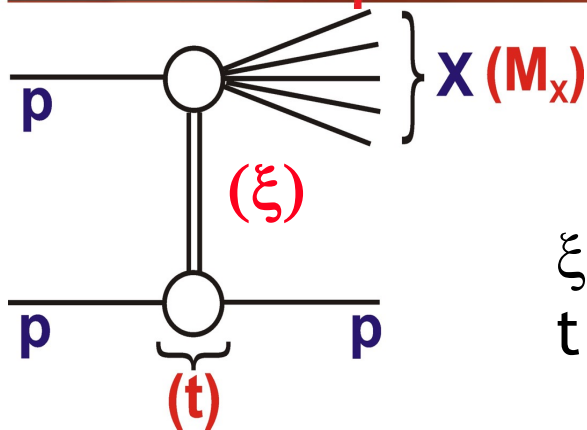
LHC beam



Geometric acceptance:

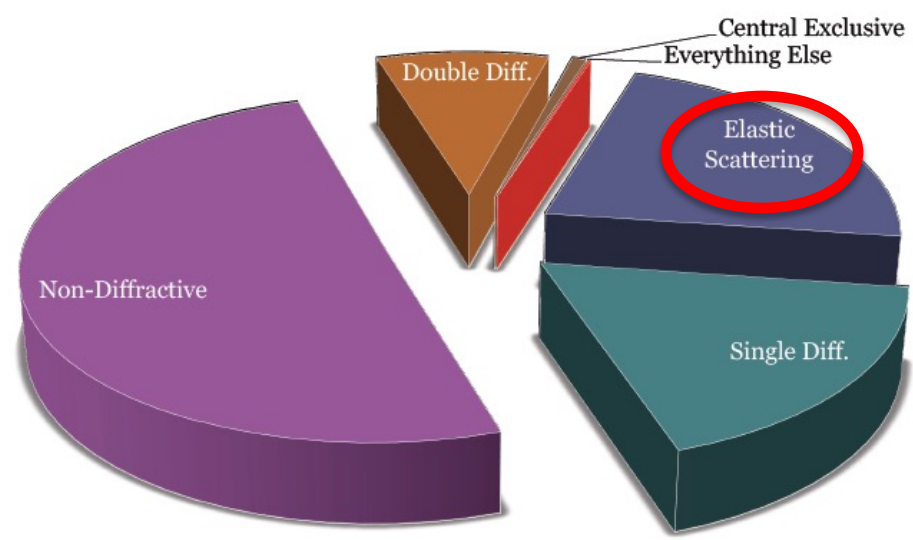
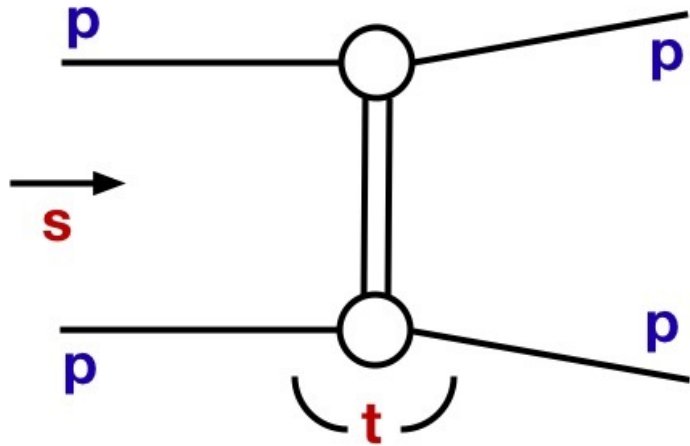


Described here in terms of kinematics of 'Single Diffractive Dissociation' (SD)



ξ = fractional proton energy loss
 $t = -p_T^2$ of outgoing proton

Start 'Simple': Elastic Scattering



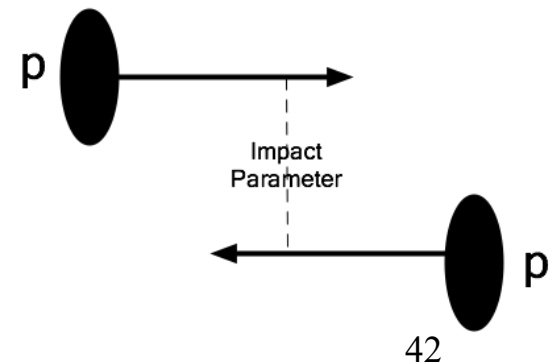
At fixed \sqrt{s} , 1 non-trivial variable
 \rightarrow squared 4-momentum transfer, t

Typically $|t| \ll 1 \text{ GeV}^2$: non-perturbative

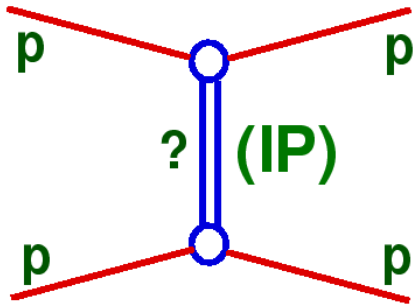
At fixed s :

$$\frac{d\sigma}{dt} = \frac{d\sigma}{dt} \Big|_{t=0} e^{Bt}$$

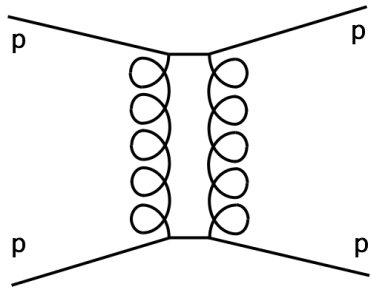
Slope parameter B measures mean impact parameter (~size of interaction region ~ range of strong force ~1-2fm).



Universal Exchange Picture of Elastic and Diffractive Scattering



- Regge asymptotics offers unified picture in terms of trajectory exchanges
- Soft 'Pomeron' dominates for sufficiently large \sqrt{s} .
- Non-perturbative object, but in Perturbative limits, loosely interpreted as exchange of two gluons in net colour singlet state, and ultimately BFKL pomeron



SOFT Pomeron trajectory:

$$\alpha(t) = \alpha(0) + \alpha' t \approx 1.085 + 0.25t$$

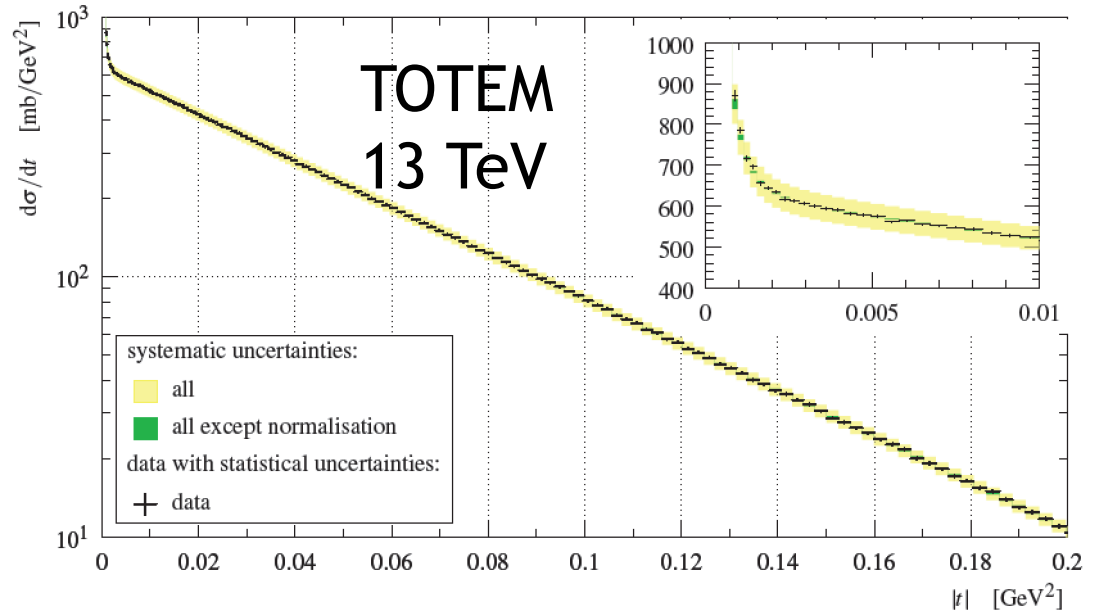
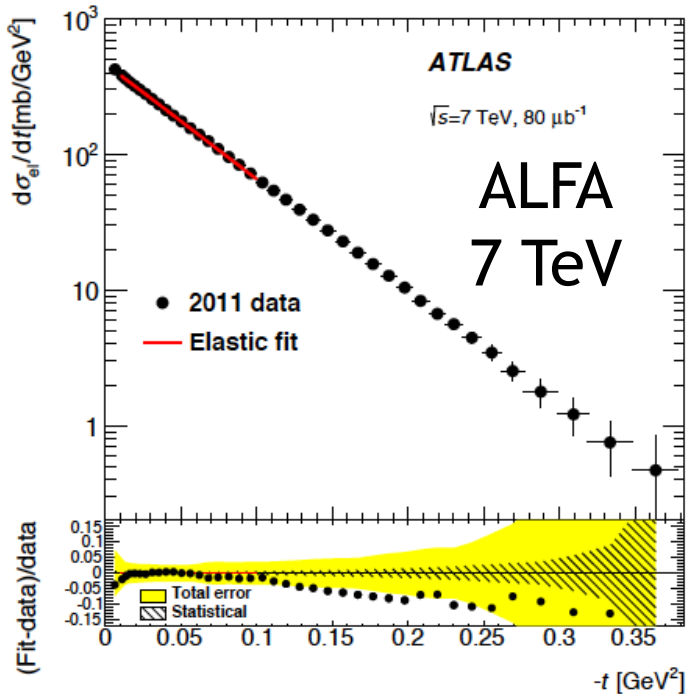
For elastic scattering:
$$\frac{d \sigma_{EL}}{d t} = \left(\frac{s}{s_0} \right)^{2\alpha(t)-2} e^{Bt}$$

... Leads to slope parameter growing logarithmically with energy

$$B = B_0 + 2\alpha' \ln \left(\frac{s}{s_0} \right) \quad 43$$

Example Elastic Scattering Data

Precise t dependence over low $|t|$ range at LHC ...



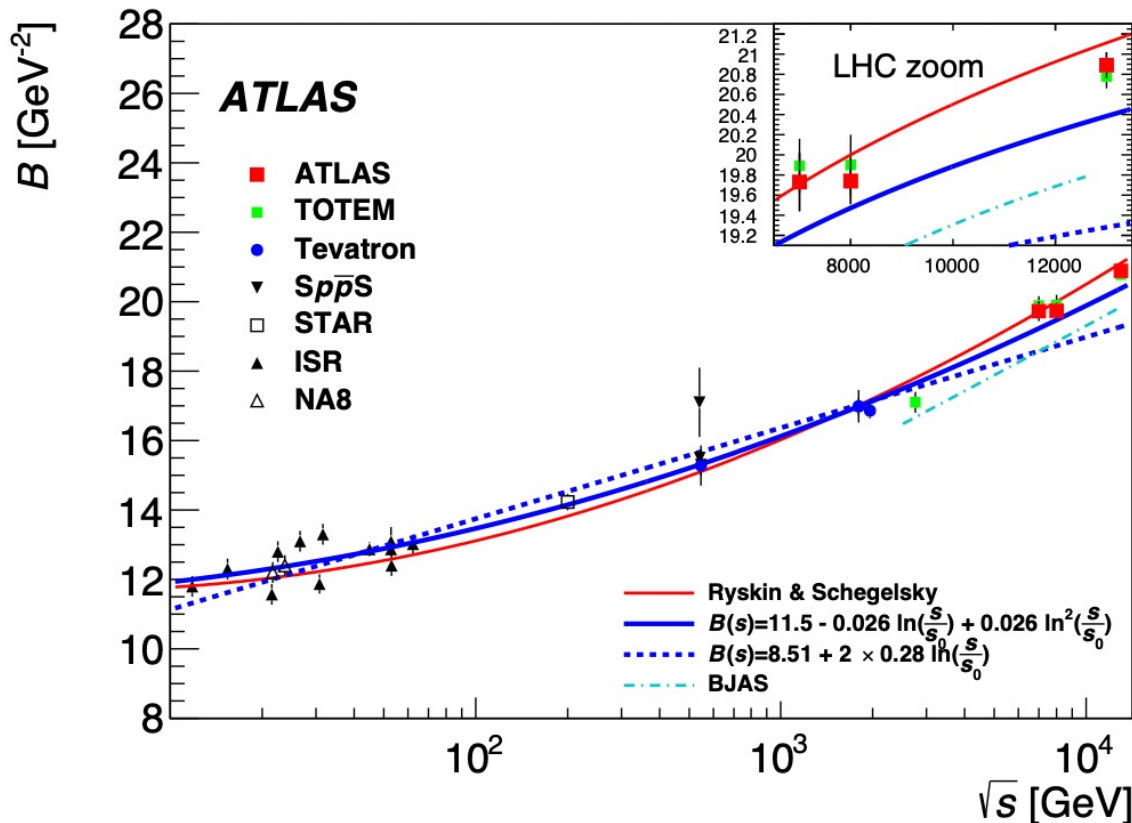
‘Standard’ exponential fit, excluding lowest $|t|$ (influence of Coulomb scattering) and largest $|t|$ (deviations, perhaps due to pQCD effects)

$$\frac{d\sigma}{dt} = \frac{d\sigma}{dt} \Big|_{t=0} e^{Bt}$$

e.g. at $\sqrt{s}=13$ TeV ... $B=21.14 \pm 0.2413 \text{ GeV}^{-2}$ (ALFA)

\sqrt{s} dependence of t Slopes

- B increases with \sqrt{s} ... 'shrinkage' of forward elastic peak \rightarrow
- ... increase of mean impact parameter / effective proton size as longer-lived fluctuations develop larger transverse size.



From fits at fixed s :

$$\frac{d\sigma_{EL}}{dt} \propto \exp(Bt)$$

'Standard' Pomeron
'pole' Regge theory

$$B = B_0 + 2\alpha' \ln\left(\frac{s}{s_0}\right)$$

- ATLAS and TOTEM
agree well

- Growth at LHC seems faster than 'standard' $\alpha' \sim 0.25 \text{ GeV}^{-2}$
- Parameterisations with \ln^2 term or more complex dependences better⁴⁵
- ... Single pomeron exchange insufficient (multi-IP / absorptive corrections)

From Elastic to Total Cross Sections

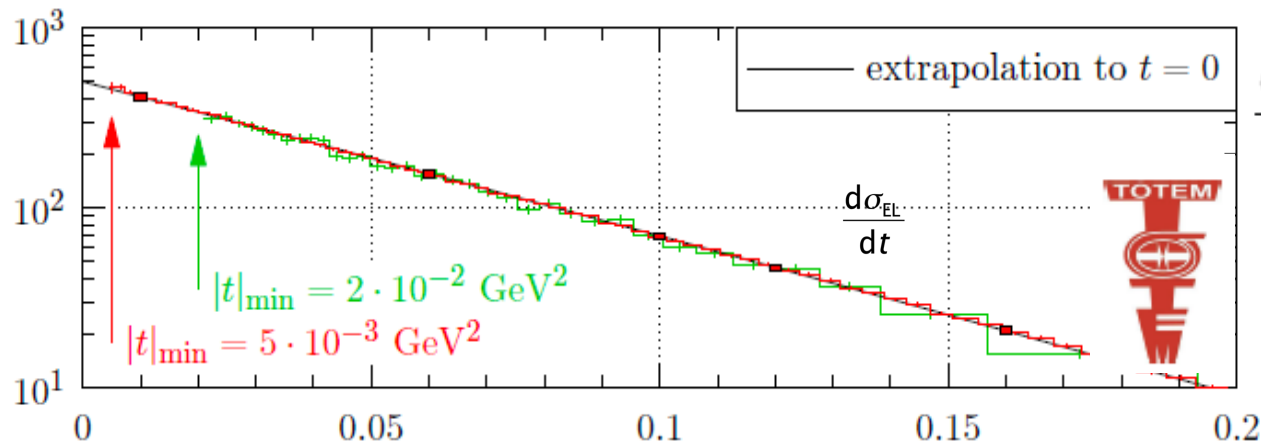
Elastic amplitude closely related to total x-sec via optical theorem ...

$$\sigma_{TOT}^2 = \frac{16\pi(\hbar c)^2}{1 + \rho^2} \cdot \left. \frac{d\sigma_{EL}}{dt} \right|_{t=0}$$

[$\rho \sim 0.1$ = Real / Imaginary part of hadronic amplitude at $t=0$]

In Regge language, leads to $\sigma_{tot} \propto \left(\frac{s}{s_0} \right)^{\alpha(0)-1}$

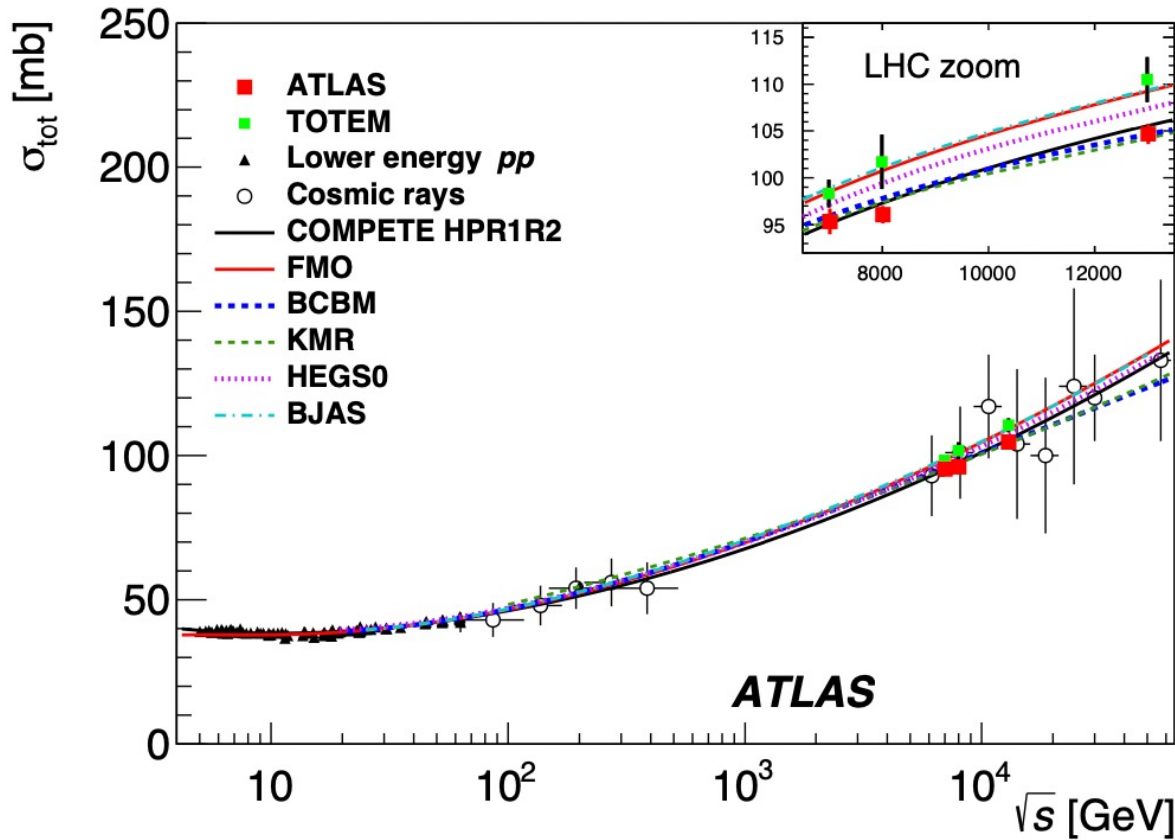
[But beware: Asymptotically (Froissart bound) limited to $\ln^2 s$ dependence]



$\left. \frac{d\sigma_{EL}}{dt} \right|_{t=0}$ obtained through extrapolation of hadronic part of elastic cross section (~10% extrapolation)

More sophisticated treatment exploits Coulomb-Nuclear interference and fit full t range, simultaneously extracting σ_{tot} and ρ ... see later

Total Cross Section versus \sqrt{s}



- Growth is slower than Regge pole power-law prediction.

- e.g. COMPETE prediction based on fits to lower energy data with multi-IP exchanges, leading to $\ln s$ and $\ln^2 s$ terms

- Systematic differences between ALFA and TOTEM arise from normalisations of elastic data.

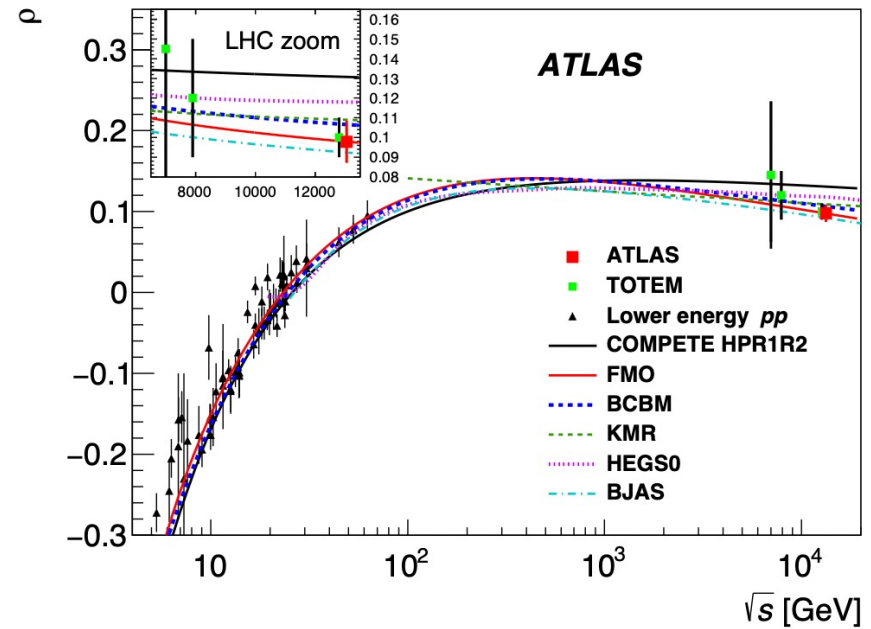
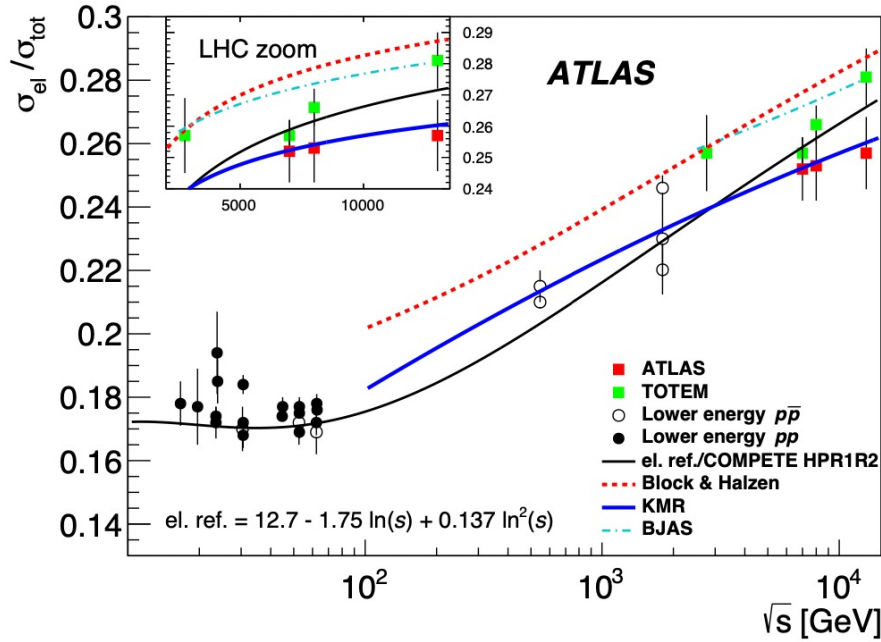
Cosmic ray data extend to 50 TeV!

data	method	ρ	σ_{tot} [mb]
$\beta^* = 90\text{m}$	Ref. [6]	-	110.6 ± 3.4
$\beta^* = 2500\text{m}$	approach 1	0.09 ± 0.01	111.8 ± 3.2
	approach 2	0.09 ± 0.01	111.3 ± 3.2
	approach 3	$0.08(5) \pm 0.01$	110.3 ± 3.5
	approach 3 (single fit)	0.10 ± 0.01	109.3 ± 3.5
$\beta^* = 90$ and 2500m	Ref. [6] \oplus approach 3		110.5 ± 2.4

[TOTEM
13 TeV]

c.f. ALFA 13 TeV: $\sigma_{tot} = 104.7 \pm 1.1\text{mb}$.

Some Low-x Implications of Elasticity

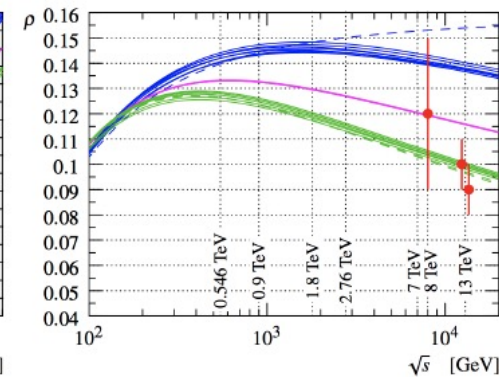
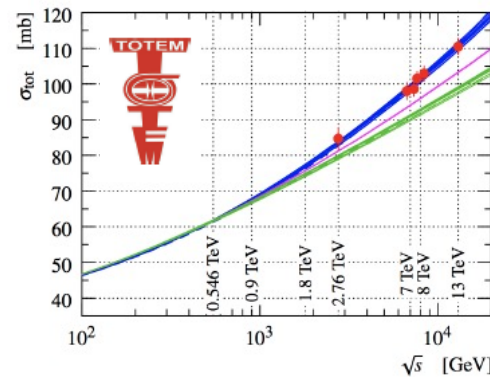


- Ratio of elastic to total cross section grows with \sqrt{s} ... related to low-x parton density growth

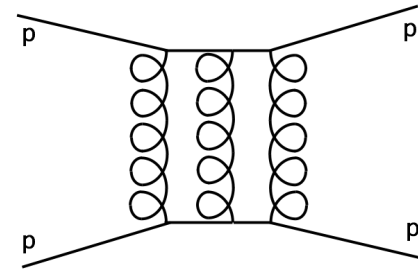
- Reaches ~ 0.26 at LHC.
c.f. Black disk limit is 0.5

- ρ parameter precisely extracted.
- TOTEM interpret failure of models to simultaneously describe ρ and σ_{tot} as evidence for C- odderon exchange

(RR)^dPL2 (20), (RR)^dPL2_u (17), (RR)^dPL2_u (19), (RR)^dP^qcL2_u (16), (RR_c)^dPL2_u (15), (RR_c)^dP^qcL2_u (14), RRPL2_u (19),
 RRP_u^fL2_u (21)
 RRPE_u (19)
 R^qcR_cL2^qc (12), RR_cL2^qc (15), RRL2 (18), RRL2^qc (17)
 R^qcR_cL^qc (12), R^qcRL^qc (14), RR_cPL (19), RR_cPL (19), RRL (18), RRL_u^f (19), RRL^qc (17), RRPL (21)
 RR(PL2) (20), RR(PL2)^qc (18)

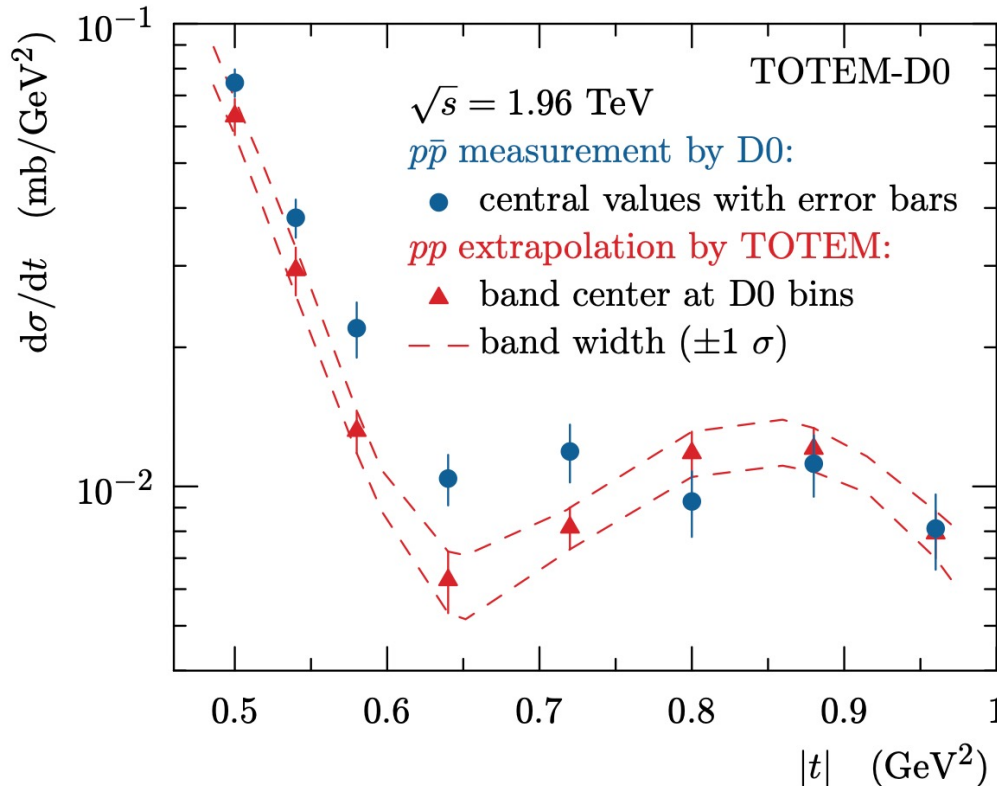


Odderons and pp versus ppbar



- CP-odd odderon exchange would contribute oppositely in pp (eg LHC) and ppbar (eg Tevatron) as $s \rightarrow \infty$.
→ smoking gun signature ...

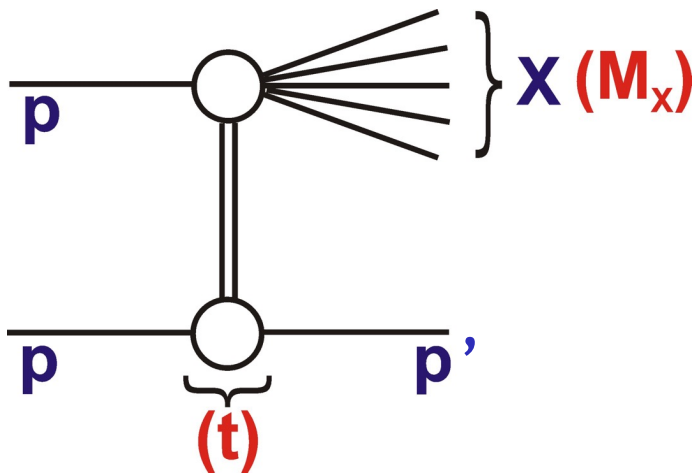
LHC (TOTEM) elastic scattering data extending to large $|t|$ ('diffractive dip') extrapolated from 2.76 TeV v Tevatron (D0) at 1.96 TeV



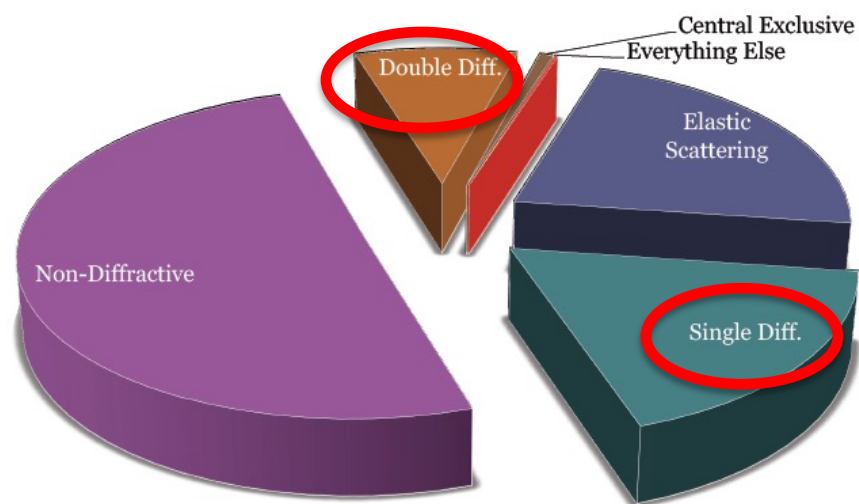
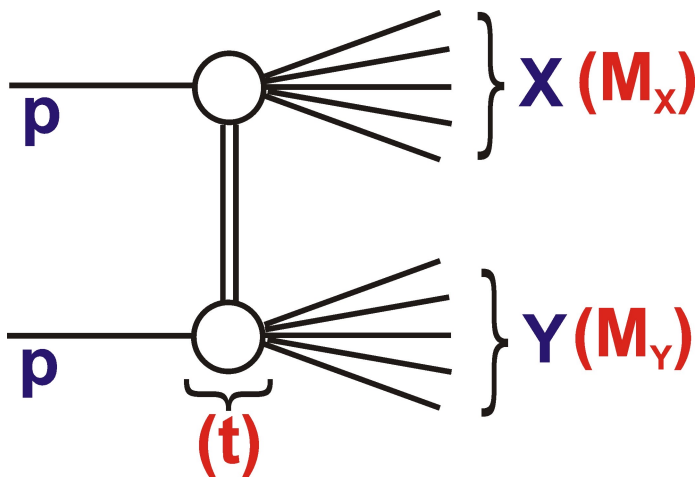
- Difference between pp and ppbar at $>3\sigma$ level
- Together with TOTEM σ_{tot} and ρ results (also $>3\sigma$), presented as an Odderon discovery
- See Valery Khoze lectures for a full discussion

Inelastic Diffraction

Single diffractive dissociation



Double diffractive dissociation



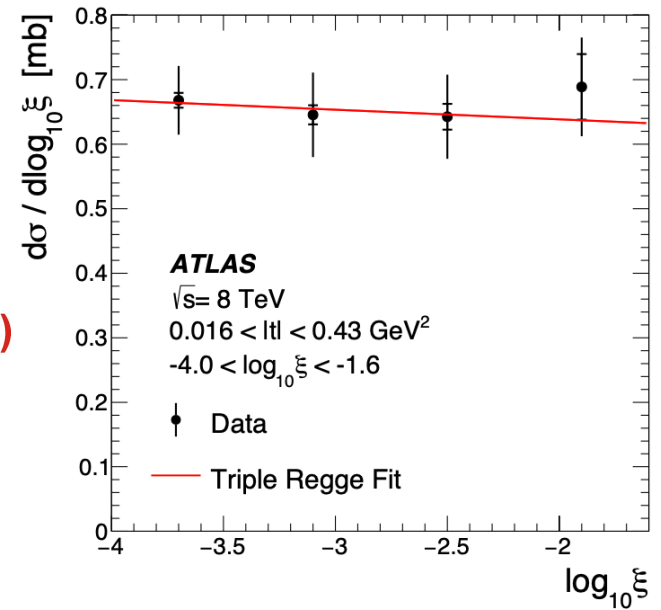
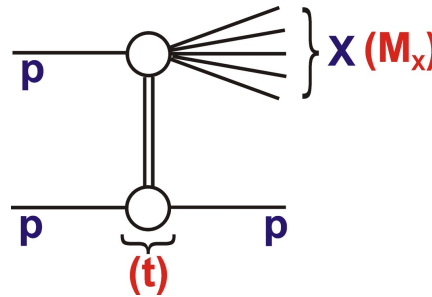
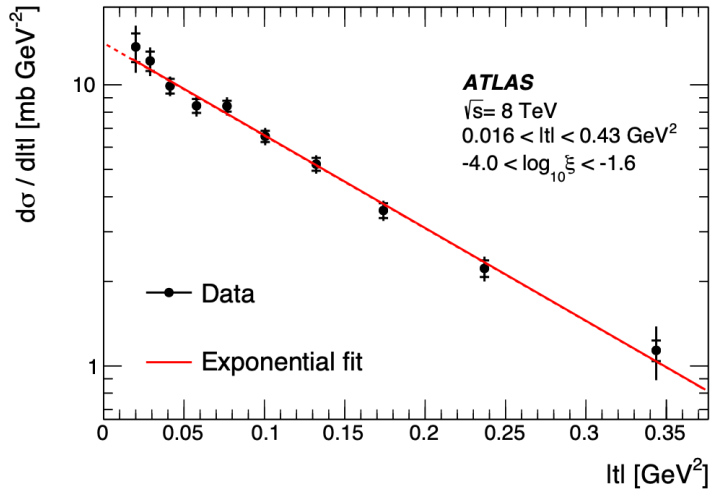
Additional kinematic variables:

$$\xi_X = \frac{M_X^2}{s} = 1 - \frac{E'_p}{E_p}$$

$$\xi_Y = \frac{M_Y^2}{s}$$

At LHC, M_X , M_Y can be as large as 1 TeV in soft diffractive processes

Proton-tagged Single Diffraction (ALFA)



- Only one published measurement [$pp \rightarrow pX$ with $\xi = M_X^2/s$]

- Interpreted in Regge theory ('Triple Regge') ...
At fixed s , with the same universal pomeron as that describing elastic cross sections ...

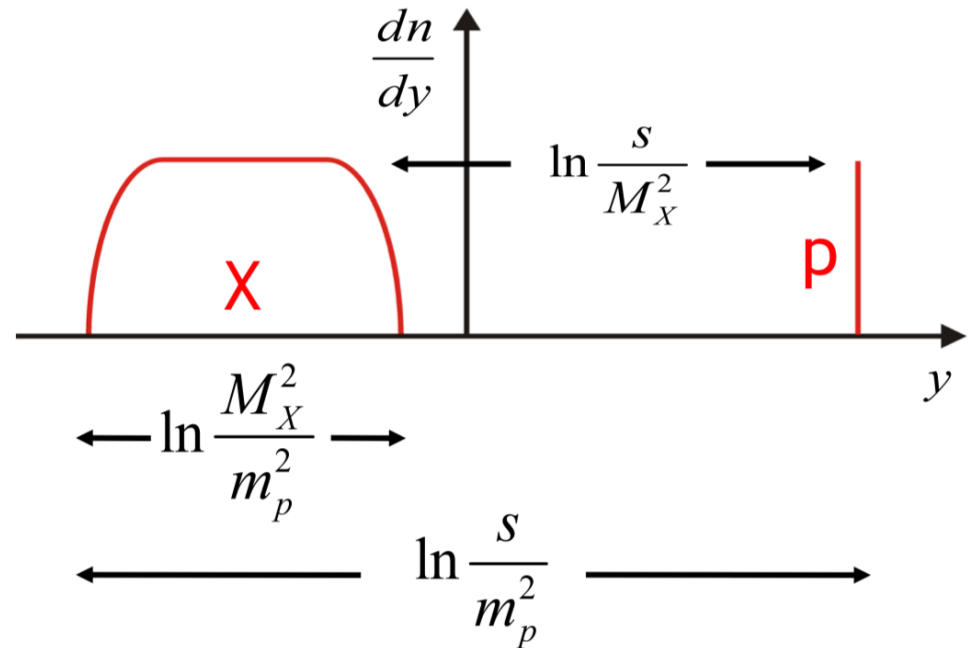
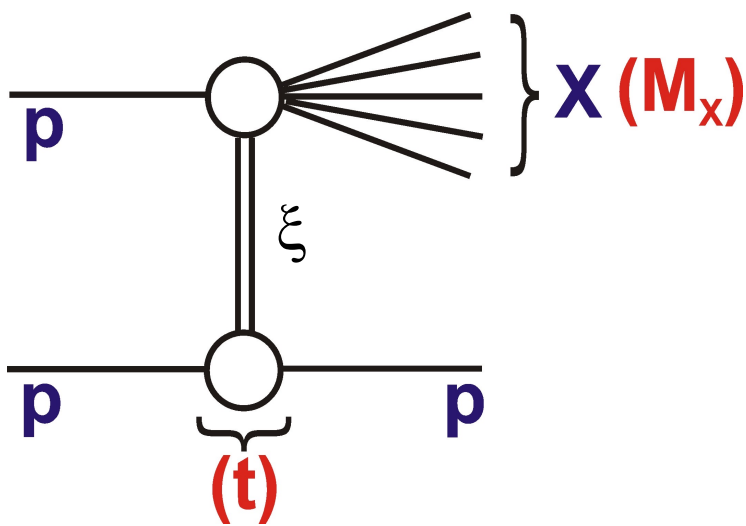
$$\frac{d\sigma}{d\xi dt} \propto \left(\frac{1}{\xi} \right)^{2\alpha(t) - \alpha(0)} e^{bt}$$

- Fitting the data yields consistent results with soft pomeron, but with large uncertainties

$$\alpha(0) = 1.07 \pm 0.02 \text{ (stat.)} \pm 0.06 \text{ (syst.)} \pm 0.06 \text{ } (\alpha')$$

$$B = 7.65 \pm 0.26 \text{ (stat.)} \pm 0.22 \text{ (syst.) GeV}^{-2}$$

Diffractive Channels: & Rapidity Gap Kinematics

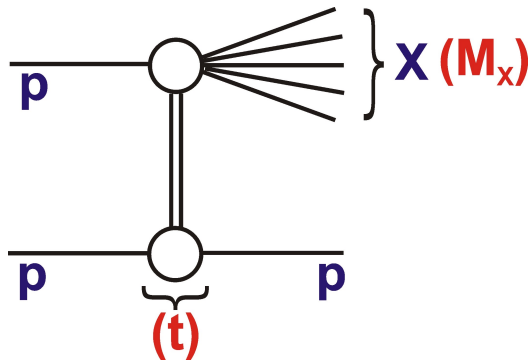
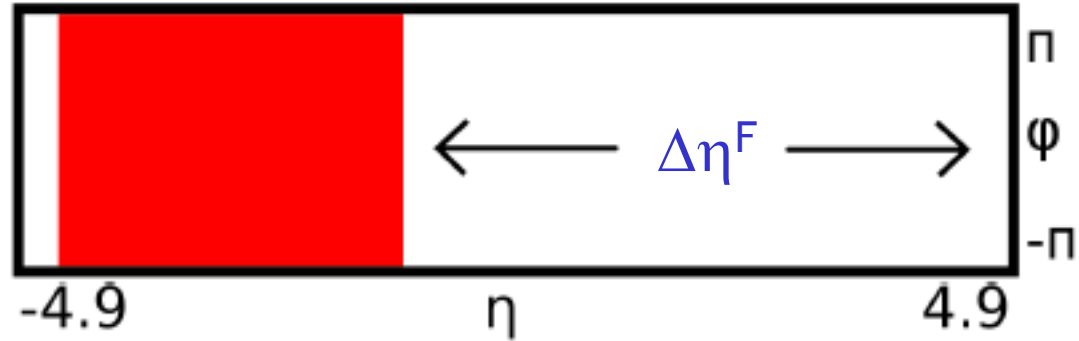


- $\xi = M_X^2/s$ is strongly correlated with $\Delta\eta \approx -\ln\xi$
empty rapidity regions
... exploited in SD measurements

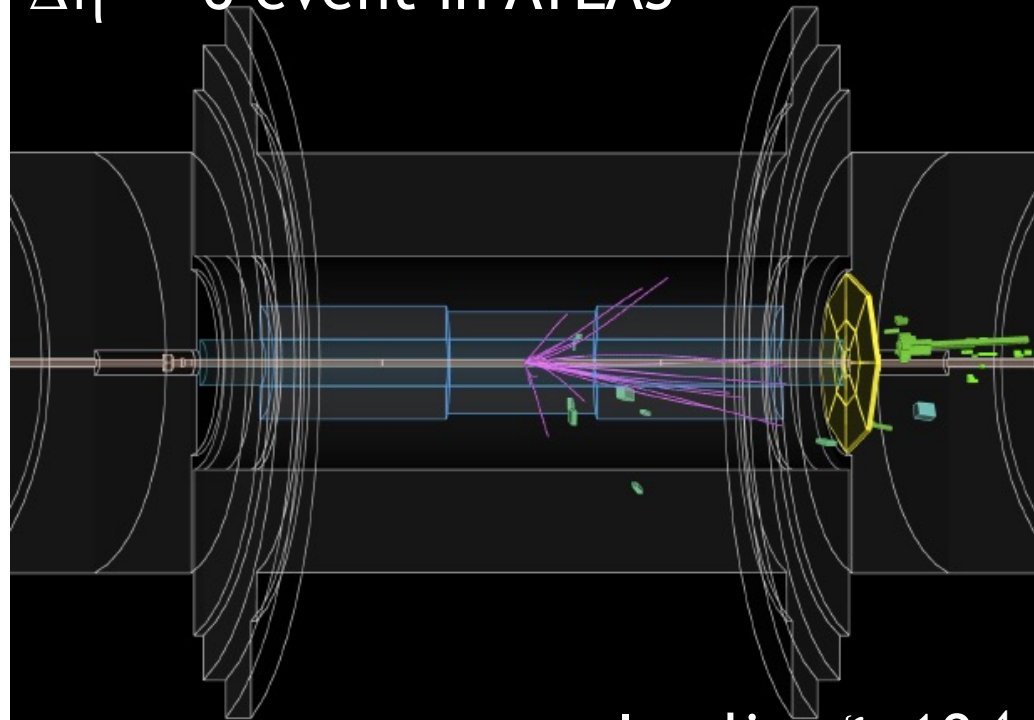
[Correlation limited by hadronisation fluctuations]

Rapidity gap cross-sections

Method developed by ATLAS to measure hadron level cross section as a function of $\Delta\eta^F$: forward rapidity gap extending to limit of instrumented range: i.e. including $\eta = \pm 4.9$



$\Delta\eta^F \sim 6$ event in ATLAS



Implies $\xi \sim 10^{-4}$

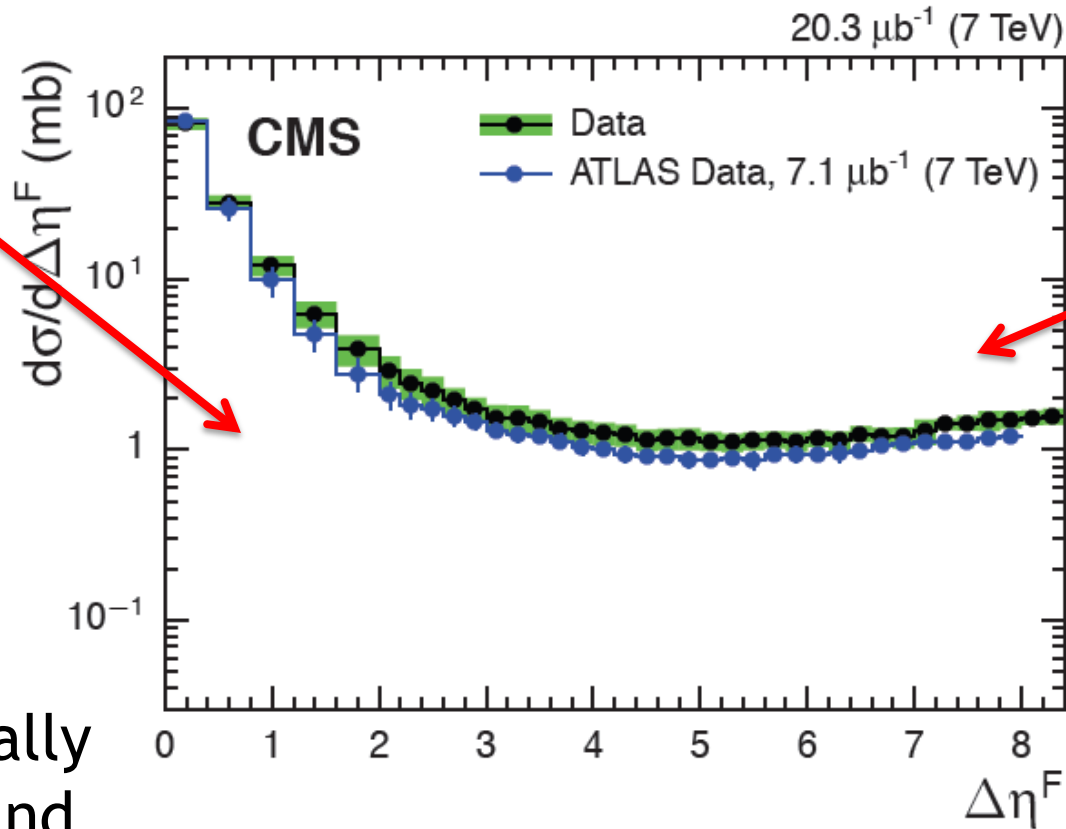
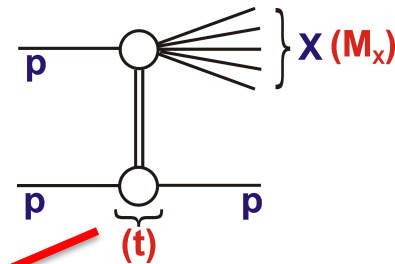
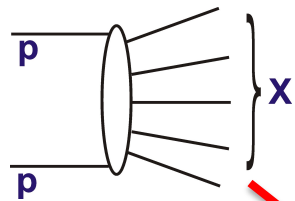
... no statement on $|\eta| > 4.9$
 ... large $\Delta\eta^F$ sensitive to
 SD + low M_Y DD

CMS and ATLAS Rapidity Gap Data

- Using very early LHC runs at 7 TeV (avoiding pile-up) ...

ATLAS: $\Delta\eta^F$ extends from $\eta = \pm 4.9$ to 1st particle with $p_t > 200$ MeV

- CMS: $\Delta\eta^F$ extends from $\eta = \pm 4.7$ to 1st particle with $p_t > 200$ MeV

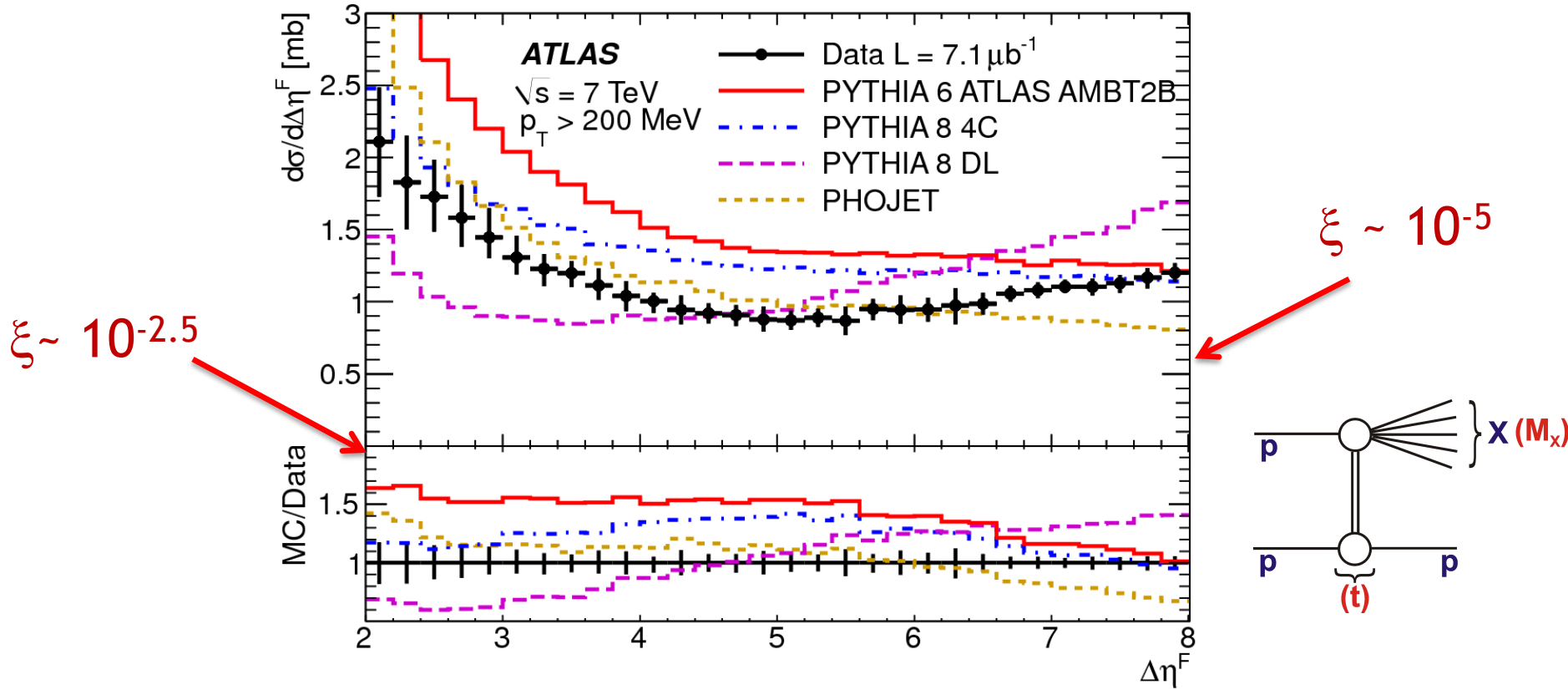


Small gaps dominated by non-diffractive processes
 ... exponentially suppressed and sensitive to hadronisation fluctuations / underlying event

Large gaps dominated by diffractive processes ... characteristic plateau

Roughly 1mb per unit gap size

Large Gap Region compared with Models



- Large differences between Monte Carlo models due to assumptions on total diffractive cross sections, $\alpha(t)$ and fragmentation modelling.

- Fit to large $\Delta\eta^F$ data using $\Delta\eta \sim -\ln \xi$ relation and $\alpha_{iP}(0) = 1.058 \pm 0.003 \text{ (stat)} \pm 0.036 \text{ (syst)}$ $\frac{d\sigma}{d\xi dt} \propto \left(\frac{1}{\xi}\right)^{2\alpha(t)-\alpha(0)} e^{bt}$

... still consistent with soft pomeron ...

Current and Future Diffraction at LHC

- Most of the ongoing diffractive programme involves Roman Pot tagging in normal high luminosity running conditions

→ Studies with double proton tags ($pp \rightarrow ppX$)

- Inclusive central production

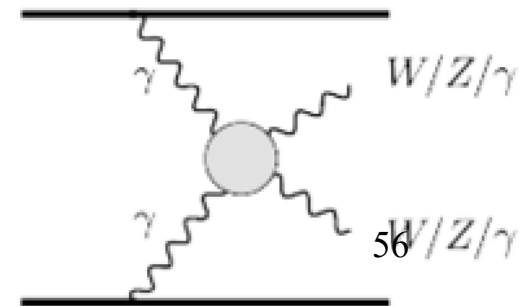
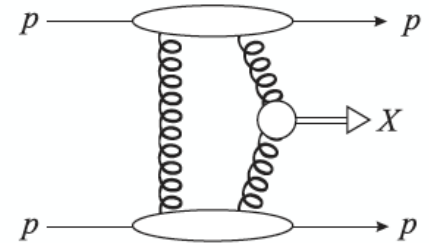
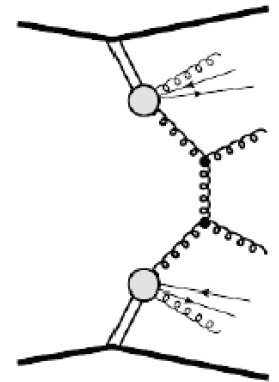
pomeron-pomeron hard scattering with jets, HF, W, Z signatures

- Central Exclusive QCD Production

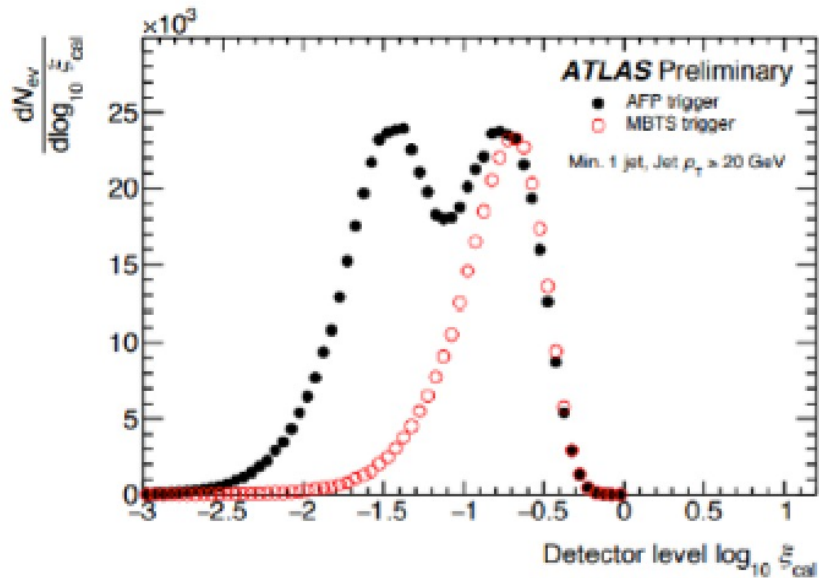
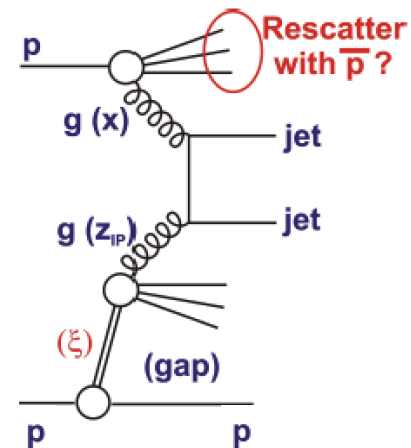
of dijets, γ -jet and other strongly produced high mass systems ... Higgs?...

- Two photon physics → exclusive dileptons, dibosons & anomalous multiple gauge couplings ...

[Dominates at large masses]



AFP Observation of Single Diffractive Dijet Signal

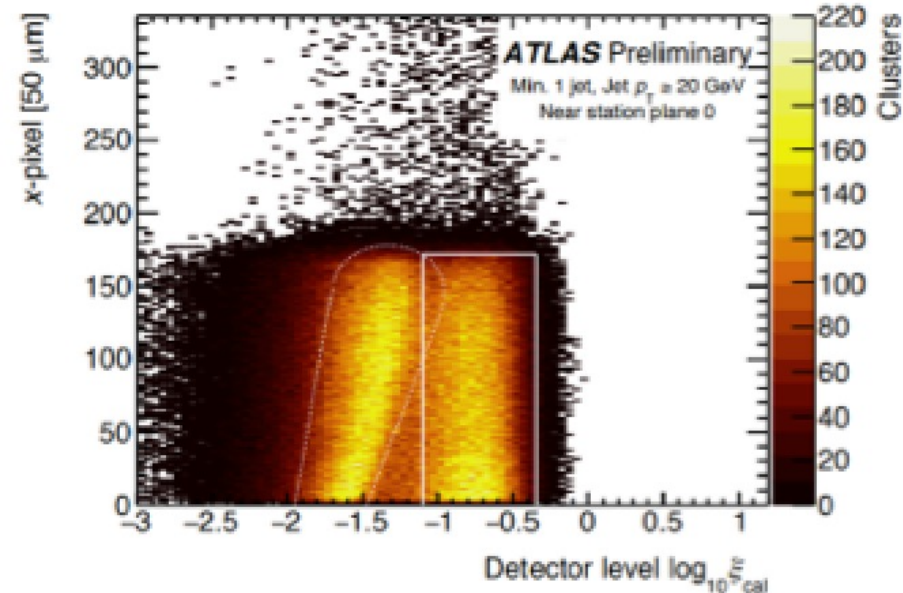


- Single proton tagged sample with ξ measured in main ATLAS calorimeter

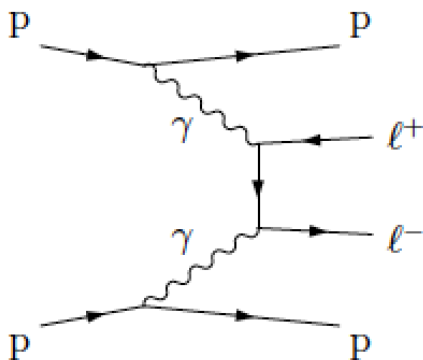
- Strong enhancement in low ξ_{Cal} diffractive region for AFP-triggered data over MBTS data + common pile-up contribution

Low ξ data exhibit expected x-y correlation in AFP pixels and correlation between pixel x position and ξ_{Cal}

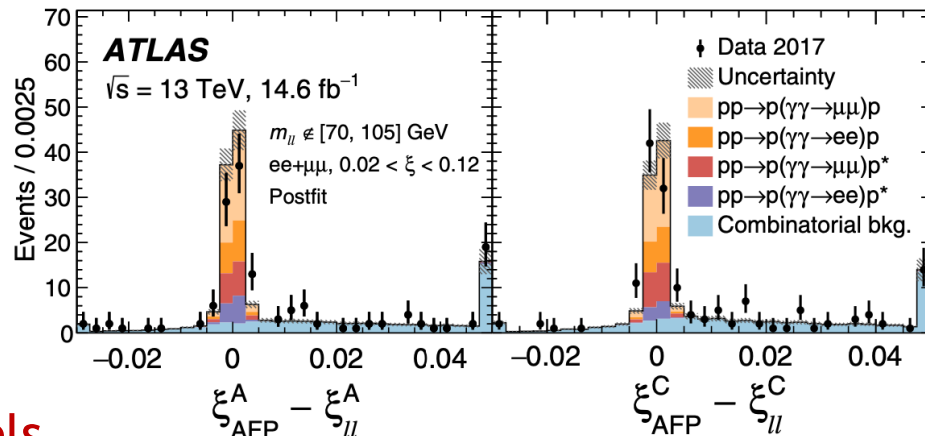
→ Clear diffractive signature



First Publications on $\gamma\gamma$ Process



Correlation between x measured In Roman Pots v Central Detectors



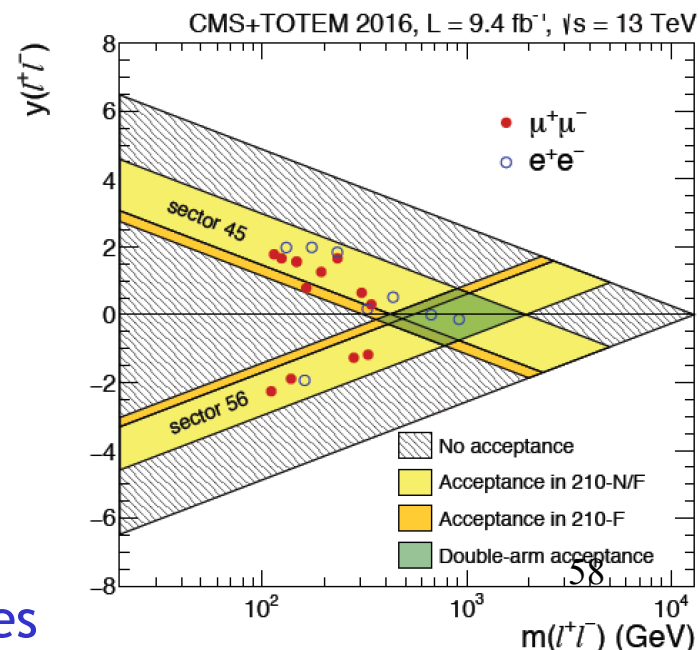
- 5σ observations by CMS-PPS and ATLAS-AFP in ee and $\mu\mu$ channels

- Dilepton masses \rightarrow TeV scale

- First (ATLAS) cross-section measurements consistent with calculations

$\sigma_{\text{HERWIG+LPAIR}} \times S_{\text{surv}}$	$\sigma_{ee+p}^{\text{fid.}}$ (fb)	$\sigma_{\mu\mu+p}^{\text{fid.}}$ (fb)
$S_{\text{surv}} = 1$	15.5 ± 1.2	13.5 ± 1.1
S_{surv} using Refs. [33,34]	10.9 ± 0.8	9.4 ± 0.7
SUPERCHIC 4 [97]	12.2 ± 0.9	10.4 ± 0.7
Measurement	11.0 ± 2.9	7.2 ± 1.8

Di-lepton rapidity versus mass



\rightarrow See Valery and Christophe's lectures

Summary

- Bulk data at LHC is a laboratory for soft strong interactions
 - Rich phenomenology of non-diffractive processes, but hard to extract underlying dynamics
 - Gaps between jets provide some evidence for BFKL
 - Elastic and diffractive data broadly as expected from soft-Pomeron Regge predictions, but with need for multi-pomeron exchanges.
 - Not yet at black disk limit, but σ_{EL}/σ_{TOT} within factor ~ 2

Next Lecture

- Diffraction at the parton level \rightarrow Diffractive DIS and Ultra-peripheral LHC Collisions
- Prospects with Future ep Colliders